TRANSCRIPTION FACTOR ZTF-22 REGULATES OXIDATIVE STRESS RESPONSES IN *CAENORHABDITIS ELEGANS*

FOZIA SALEEM

A THESIS SUBMITTED TO THE FACULTY OF GRADUATE STUDIES
IN PARTIAL FULFILLMENT OF THE REQUIREMENTS FOR THE
DEGREE OF MASTER OF SCIENCE

GRADUATE PROGRAM IN BIOLOGY
YORK UNIVERSITY
TORONTO, ONTARIO

FEBRUARY 2023

Abstract

Oxidative stress is caused when the balance between Reactive Oxygen Species (ROS) and detoxification enzymes is disturbed. In *Caenorhabditis elegans* (*C. elegans*), *gst-4* is an important detoxification enzyme that is activated by the SKN-1 transcription factor when the cell experiences oxidative stress. Our lab previously showed that SKN-1 is negatively regulated by BRAP-2 and *brap-2* mutants show elevated levels of *gst-4.* Our lab performed RNAi screening and found that the knockdown of another transcription factor, ZTF-22, also enhanced *gst-4* levels. Therefore, ZTF-22 was selected for further investigation in the context of oxidative stress. I found that loss of ZTF-22 caused an increased expression of *gst-4*, and *sod-3*. I also found that *ztf-22* deletion caused lifespan extension, reduced survival under heat stress and increased survival under the ER stress. Therefore, ZTF-22 contributes to the oxidative stress response, but also plays biological roles in thermotolerance, longevity, and the ER stress response.

Acknowledgements

All the praise and gratitude belong to **ALLAH**, the most Gracious, the most Merciful, the Creator of everything, the One and Only, the Everlasting. I could never thank You enough for blessing me with the best of everything.

I would like to thank my esteemed supervisor, **Dr. Terrance J. Kubiseski**, for taking me under your supervision and letting me conduct research in your lab. You are an amazing human being and a wonderful teacher and mentor. You have helped me become a researcher; I owe my entire research career to you. You have been very accommodating especially when I hit a rough patch in my life. I couldn't have asked for a better teacher.

Next, I would like to thank my advisor, **Dr. Patricia Thomas-Lakin**. Your critical feedback has helped me tremendously in becoming a better researcher. You always asked me question that kept me from digressing and helped me stay on track.

I would like to thank **Magdalena Jaklewicz** for teaching me how to use the Confocal microscope and teaching me new techniques for taking beautiful pictures of my worms.

I would like to extend my gratitude to my lab colleagues, Cindy Tran, Alessia Libertucci, and our new undergraduate lab members, Rawan and Aaron. **Cindy**, thank you very much for welcoming me into the lab and teaching me all the lab techniques, without you I would have been completely lost. **Alessia**, thank you very much for being such a wonderful friend and colleague. You have always made my day more enjoyable and cheerful. Thank you for taking care of my worms and doing labwork for me when I was away. You are awesome!! **Rawan** and **Aaron**, I wholeheartedly welcome you to our lab and hope you will have a great time. I would also like to thank **Farnaz** and **Esra** for helping me with qPCR stats whenever I got stuck.

I am eternally grateful for being blessed with wonderful parents**, Muhammad Saleem** and **Fahmida Bibi,** and my siblings. I could never in my thousand lives pay for all the support and unconditional love that you have shown me. To my siblings, you guys know exactly how to get on my nerves, but honestly I cannot imagine my life without you, so thank you for making my life more entertaining.

Lastly, to the hundreds of **worms** that lost their lives during this research, I appreciate the sacrifice.

Table of Content

List of Figures

List of Tables

List of Abbreviations

AAKG-4	AMP-Activated protein Kinase Gamma subunit
ADP	Adenosine diphosphate
AMP	Adenosine monophosphate
AMPK	AMP-activated protein kinase
ARE	Antioxidant response element
As	Sodium Arsenite
ATP	Adenosine Triphosphate
BRCA	Breast cancer
bZIP	Basic-leucine zipper
C. elegans	*Caenorhabditis elegans*
C2H2	$Cystein_2/Histidine_2$
CGC	Caenorhabditis Genetics Center
CTL	CaTaLase
CUL4	CULin
DDB	DNA damage-binding
DDL	Daf-16-dependent longevity
DNA	Deoxyribonucleic Acid
DOD	Downstream of DAF-16
DTT	Dithiothreitol
E. coli	*Escherichia coli*
EGF	External growth factor
ELT	Erythroid-Like Transcription factor family
ER	Endoplasmic Reticulum
ERK	Extracellular signal-regulated protein kinases
Fe^{2+}	Reduced iron
FMO	Flavin monooxygenase
FOXO	Forkhead Box
FTT	Fourteen-Three-Three family
GDP	Guanine diphosphate
GEF	Guanine Exchange Factor
GPX	Glutathione peroxidase
GR	Glutathione reductase
GSH	Glutathione
GST	Glutathione S-transferase
GTP	Guanine Triphosphate
H_2O_2	Hydrogen peroxide
IIS	Insulin/IGF-like signaling
ILPs	Insulin-like peptides
INS	INSulin related
JKK	JNK Kinase

JNK	c-Jun N-terminal Kinase
Keap1	Kelch-like ECH-associated protein 1
KSR	kinase suppressor of Ras
LIN	abnormal cell LINeage
MAPK	Mitogen-Activated Protein Kinase
MAPKK	Mitogen-Activated Protein Kinase Kinase
MAPKKK	Mitogen-Activated Protein Kinase Kinase Kinase
MEK	MAP kinase kinase or Erk Kinase
MPK	Map Kinase
mRNA	messenger RNA
MTL	MeTaLlothionein
NADPH	Nicotinamide adenine dinucleotide
NGM	Nematode Growth Medium
NSY	Neuronal SYmmetry
O_2^-	Superoxide radical
OH^-	Hydrogen peroxide radical
$OH^\cdot$	Hydroxyl radical
PAR	abnormal embryonic PARtitioning of cytoplasm
PCR	Polymerase Chain Reaction
PDK	PDK-class protein kinase
PI and PII	Phase I and Phase II
PIK3	Phosphoinositide 3 kinase
PMK	P38 Map Kinase family
PPTR	Protein Phosphatase 2A (Two A) Regulatory subunit
PTEN	phosphatase and tensin homolog
qRT-PCR	quantitative Real Time- PCR
Raf	Rapidly accelerated fibrosarcoma
Ras	Rat sarcoma oncogene
RNA	Ribonucleic Acid
RNAi	RNA interference
ROS	Reactive Oxygen Species
RTK	Receptor Tyrosine Kinase
RTK	Tyrosine kinase receptor
SDH	Short-chain dehydrogenase
SOD	Superoxide dismutase
SW-PCR	Single Worm-Polymerase Chain Reaction
tBHP	*tert*-Butyl Hydroperoxide
TF	Transcription factor
TOR	Target of Rapamycin
WT	Wild type
YF	Kubiseski lab
ZFP	Zinc Finger Protein

CHAPTER 1: INTRODUCTION AND LITERATURE REVIEW

1.0 Introduction:

1.1 General introduction:

Aging is an inexorable process experienced by many living organisms. This process, however, is accompanied by a number of debilitating diseases that eventually lead to the death of an organism. Age-related diseases such as cancer, cardiovascular and neurodegenerative diseases are the leading causes of death in the world, especially in industrialized countries (1). These age-related diseases impose a substantial economic and psychological strain on the health care system, patients, their families, and society as a whole (1). In Ontario, for instance, the cost of treating diabetes escalated from $14 billion in 2008 to just under $30 billion in 2019 (2). Moreover, the total health care system and out of pocket costs of caring for people with dementia were $10.4 billion in 2016, and are projected to double by 2031 (3). It was estimated that in 2016 there were 564,000 persons in Canada living with dementia and by 2031 the number is estimated to increase to 937,000. These staggering numbers reflect the urgent need to find strategies to prevent or at least delay the onset of chronic age-related diseases in order to lighten the financial burden on society.

One of the major contributors to detrimental diseases associated with aging is the cellular damage caused by Reactive Oxygen Species (ROS) (4). ROS are produced as a result of oxygen metabolism. At low concentrations, they serve as important signaling molecules (5), however, their prolonged exposure can cause severe damage to DNA, proteins, and lipids (6). When there is an imbalance between the generation of ROS and the ability of detoxification enzymes to scavenge ROS, the cell is said to be under oxidative stress (7). Animal cells have developed defense mechanisms, regulated by various complex signaling pathways, to keep ROS levels under control and avoid damage caused by oxidative stress.

In order to develop therapeutic interventions required to treat age-related diseases, it is crucial to understand the signaling pathways involved in the regulation of oxidative stress. Many of these intricate signaling cascades are highly conserved and have counterparts in other organisms such as worms, mice, and flies. These simpler animals are used as model organisms to dissect complicated underlying mechanisms of various processes. In this project, I used a microscopic nematode, *Caenorhabditis elegans*, to determine the role of ZTF-22 transcription factor in the oxidative stress response.

1.1.1 *Caenorhabditis elegans* as a model organism:

In 1965, Sydney Brenner settled upon using *Caenorhabditis elegans* (*C. elegans*) as a model organism to study developmental biology and neurobiology (8,9). It was selected as a model organism because of its small size (1.5 mm long adult) with 959 somatic cells, transparent body, rapid life cycle (~3 days), and ability to self-fertilize (10). Two sexes are found in *C. elegans :* males and hermaphrodites. The hermaphrodites contain both eggs and sperms and lay fertilized eggs. A single hermaphrodite can lay up to 300 fertilized eggs. However, when male worms are present in the population, sperm from male worms are preferred for fertilization (11). This feature allows researchers to perform genetic crosses between different strains to obtain desired genotypes. In addition, various genetics tools such as the generation of transgenic worms, use of GFP to track the location of a particular protein, RNA interference to study the effect of a particular protein, qPCR to measure the RNA levels of different genes etc. are used to manipulate its simple system to study its genetics and molecular pathways.

In 1998, *C. elegans* became the very first multicellular organism to have its entire genome sequenced (12). There are between ~20,250 and ~21,700 predicted protein-coding genes in *C. elegans* (13). Many of these genes are conserved between *C. elegans* and other organisms such

as flies, mice, and humans. For instance, 70% of *C. elegans* lipid genes have human orthologs and many of these genes are directly related to human metabolic diseases (14). Because of this conservation of gene function, *C. elegans* has been used extensively to study the fundamental genetics and molecular mechanisms underlying human diseases. So far this organism has contributed to the understanding of various human pathologies such as cancer, neurodegeneration (e.g. Alzheimer's disease), neurodevelopmental disabilities and syndromes, muscular dystrophies, and the process of aging (15). In this thesis, I have used this remarkable model organism to study oxidative stress in the context of *ztf-22* mutation and the general role of *ztf-22* in terms of lifespan and survival against various stresses.

1.2 Oxidative Stress:

A cell hosts numerous chemical reactions over its lifetime. These reactions take place in various parts of the cell such as cytoplasm, mitochondria, lysosomes, etc., and are essential for the survival and growth of the organism. However, in addition to the production of important products, certain harmful by-products are also generated as a result of these reactions. One such important class of by-products released is called Reactive Oxygen Species (ROS).

ROS is a group of highly reactive oxygen particles with unpaired electrons such as superoxide anion ($\cdot O_2^-$), hydroxyl ion (OH^-), and hydroxyl radical ($OH\cdot$). At low concentrations, ROS plays a crucial role in important physiological processes but at high concentrations, it can damage important biological molecules, DNA, lipids, and proteins, thus compromising cell survival (16). To mitigate the harmful effects of ROS, the cell produces detoxification enzymes. These enzymes regulate the concentration of ROS at an appropriate level under quiescent conditions. However, when the delicate balance between ROS and detoxification enzymes is

perturbed such that ROS levels exceed normal levels, the cell is considered to be under an "oxidative stress" state.

1.2.1 ROS generation and detoxification:

There are a large number of enzymes that produce ROS, however, these four enzymatic systems in the mammalian cells predominate others in ROS productions; NADPH oxidases (17), xanthine oxidase (18), uncoupled NO synthase (19), and the mitochondrial electron transport chain (20) (Figure 1.1). To ensure efficient cell function, detoxification enzymes keep ROS levels under tight control. There are three types of detoxification enzymes; Phase I (PI) detoxification enzymes are the first ones to detoxify ROS, examples of PI detoxification enzymes include SODs, Cytochrome P450, etc. Phase II (PII) detoxification enzymes react with the by-products of PI detoxification, examples include GPX, GSTs, UGTs etc. Phase III (PIII) detoxification enzymes are responsible for removing the by-products of PI and PII detoxification from the cell, examples include ATP-binding cassette and other transporters (21).

Superoxide dismutase (SOD) is a family of PI detoxification enzymes that is responsible for removing $\cdot O_2^-$ from the cell by converting it into H_2O_2 (22). Five isoforms of SOD genes have been identified in *C. elegans* . *sod-1* and *sod-5* are cytosolic isoforms, *sod-4* encodes a membrane-bound variant and an extracellular variant whereas *sod-3* and *sod-2* are mitochondrial isoforms (23). In the presence of reduced iron (Fe^{2+}), hydrogen peroxide (H_2O_2), resulting from the dismutation of $\cdot O_2^-$, can yield the highly toxic $OH\cdot$. However, Glutathione peroxidase (GPX) or catalase catalyzes the decomposition of H_2O_2 into H_2O and O_2 by using reduced glutathione (GSH) (24). Glutathione *S*-transferase (GST) catalyzes the nucleophilic conjugation of GSH with a wide range of substrates to allow their secretion out of the cells (25).

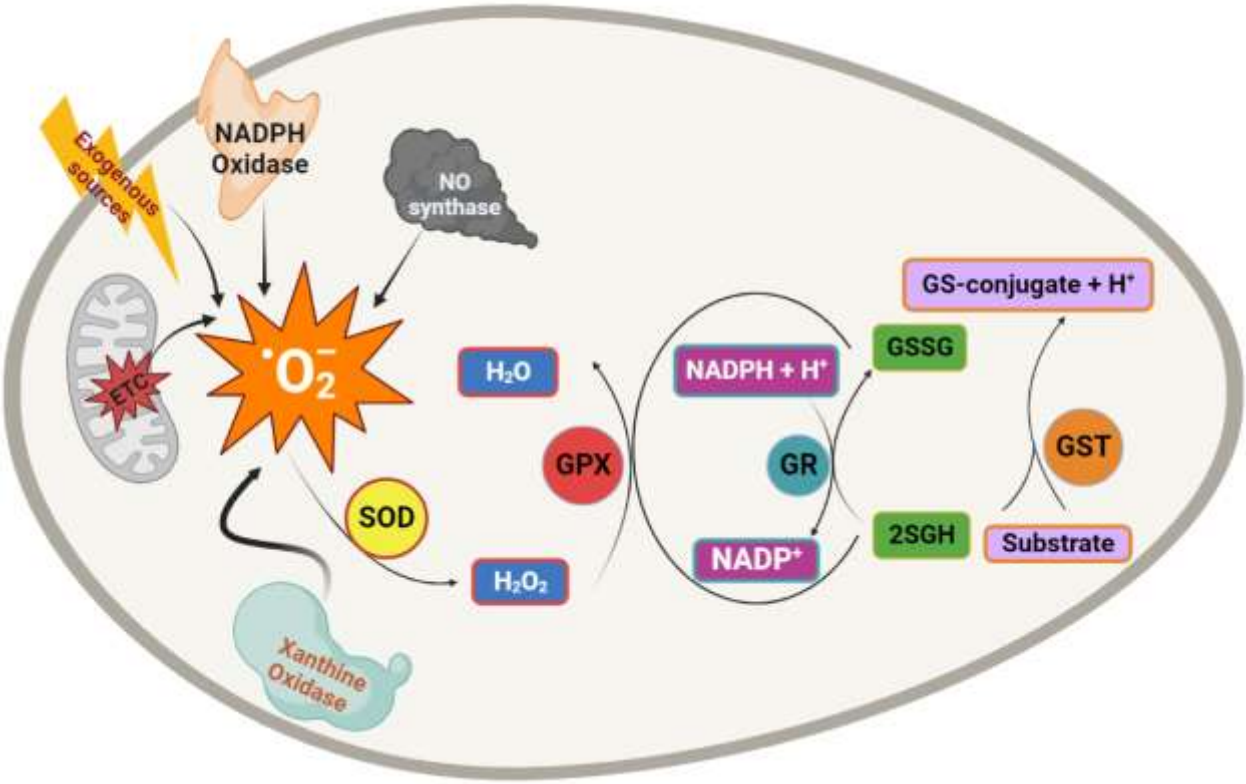

Figure 1. 1 Generation and detoxification of ROS

In the cell, ROS is produced mainly by NADPH oxidase, NO synthase, Xanthine oxidase, and mitochondrial ETC. The exogenous sources of ROS include radiation, pollutants, smoking, and diet. For simplicity, only superoxide anion ($\cdot O_2^-$) is shown to represent ROS. The superoxide anion is converted into H_2O_2 by SOD. The resulting H_2O_2 is converted into water by glutathione peroxidase (GPX) through the use of reduced glutathione (GSH). GSH is turned back to its original form by the oxidation of NADPH via glutathione reductase (GR). Glutathione-*S*-transferase (GST) catalyzes the conjugation of GSH to various substrates for their excretion from the cell. Adapted and modified from Yan *et al.*, 2008 (26)

1.2.2 Aging in *C. elegans :*

Aging is manifested by a progressive decline in the functional homeostasis of tissue maintenance and an escalating predisposition to degenerative diseases and death (27). Research shows that the risk of many chronic diseases including cancer, cardiovascular, and neurodegenerative diseases considerably increases with aging (28). It is a multifactorial process that has been extensively studied for decades and continues to be an active area of research. Oxidative stress is one of the factors that has been shown to be linked to aging. According to the free radical theory of aging, the accumulation of the detrimental impact of ROS over an organism's lifetime and its ability to deal with this damage determines its lifespan (29).

C. elegans has proven to be an excellent model for studying aging and lifespan because of its short lifespan (~3 weeks), high homology with mammals, high fertility, transparent anatomy, small size, and cheap laboratory maintenance (10). Interestingly, the discovery that aging is regulated by genetic mechanisms, like other biological processes, was first made in *C. elegans* . Many of the mutations that extend *C. elegans '* lifespan are found in the Insulin/IGF-1 signaling pathway. The key mutations in this regard are *age-1, daf-2,* and *daf-16* (the mammalian homologs of these genes are mentioned in Table 1). The mutations in *age-1* and *daf-2* not only cause lifespan extension but also increase stress resistance in worms (30–32). Dissection of these pathways in worms will pave the way for understanding the molecular mechanism underlying the intricate phenomenon of aging.

1.3 *C. elegans* Signaling Pathways involved in the Oxidative Stress Response:

Transcription factors (TFs) are important proteins that are involved in the regulation of various cellular processes. They recognize and bind specific DNA regions and can either promote or suppress the transcription of target genes (33). Many diseases including cancer, autoimmunity,

neurological disorders, diabetes, cardiovascular disease, and obesity have been shown to be caused by mutations in TFs and other proteins that directly interact with DNA (34). In *C. elegans* , more than 900 TFs from different families have been predicted (35). Some of these TFs are highly conserved as they have homologs in other animals such as members of the homeodomain, forkhead, and the zinc finger families (36). They play an important role in immune response, apoptosis, metabolism, aging, sex determination, and oxidative stress (37,38) . TF activity is tightly regulated by various signaling pathways. Many TFs and their corresponding regulatory signaling pathways are conserved between *C. elegans* and mammals. Below I discuss some important signal transduction pathways and their target transcription factors that are pertinent to my project.

1.3.1 The Insulin/Insulin-like Growth Factor Signaling Pathway:

The Insulin/IGF-1 signaling pathway (IIS) is one of the most well-known aging-regulatory pathways. Its role in metabolism, reproduction, stress resistance, and longevity is conserved from worms to humans (31,39–41). This pathway is triggered when the insulin-like peptides (ILPs) bind to the DAF-2 transmembrane receptor (the *C. elegans* IGF-1 ortholog) resulting in its activation (Figure 1.2). Once DAF-2 is activated, it recruits and activates phosphoinositide 3 kinase (AGE-1/PIK3). As a result of this, the serine/threonine kinases (PDK-1, AKT-1, and AKT-2) are activated and result in the phosphorylation of the DAF-16/FOXO transcription factor. Phosphorylation of DAF-16 regulates its interaction with 14-3-3 proteins PAR-5 and FTT-2 which are responsible for controlling its subcellular localization. The DAF-18/PTEN lipid phosphatase and the serine/threonine phosphatase PPTR-1/PP2A counteract AGE-1/PI3K and AKT-1 signaling, respectively (42).

Under standard conditions, IIS is active and keeps DAF-16 sequestered in the cytoplasm through its phosphorylation. However, under stressful conditions, phosphorylation of DAF-16 is

reduced leading to its nuclear localization. Once DAF-16 translocates to the nucleus, it binds specific promoters and regulates the transcription of its target genes which are predominantly involved in stress resistance mechanisms and promoting longevity (20,26). In addition to inhibiting DAF-16, IIS also directly inhibits another transcription factor, SKN-1 (the *C. elegans* Nrf2 ortholog) by phosphorylating it via AKT-1, AKT-2, and SGK-1. The reduced IIS leads to constitutive nuclear localization of SKN-1 ultimately contributing to increased stress resistance and longevity (45). The heat shock protein, HSF-1, is negatively regulated by the IIS pathway as well (46).

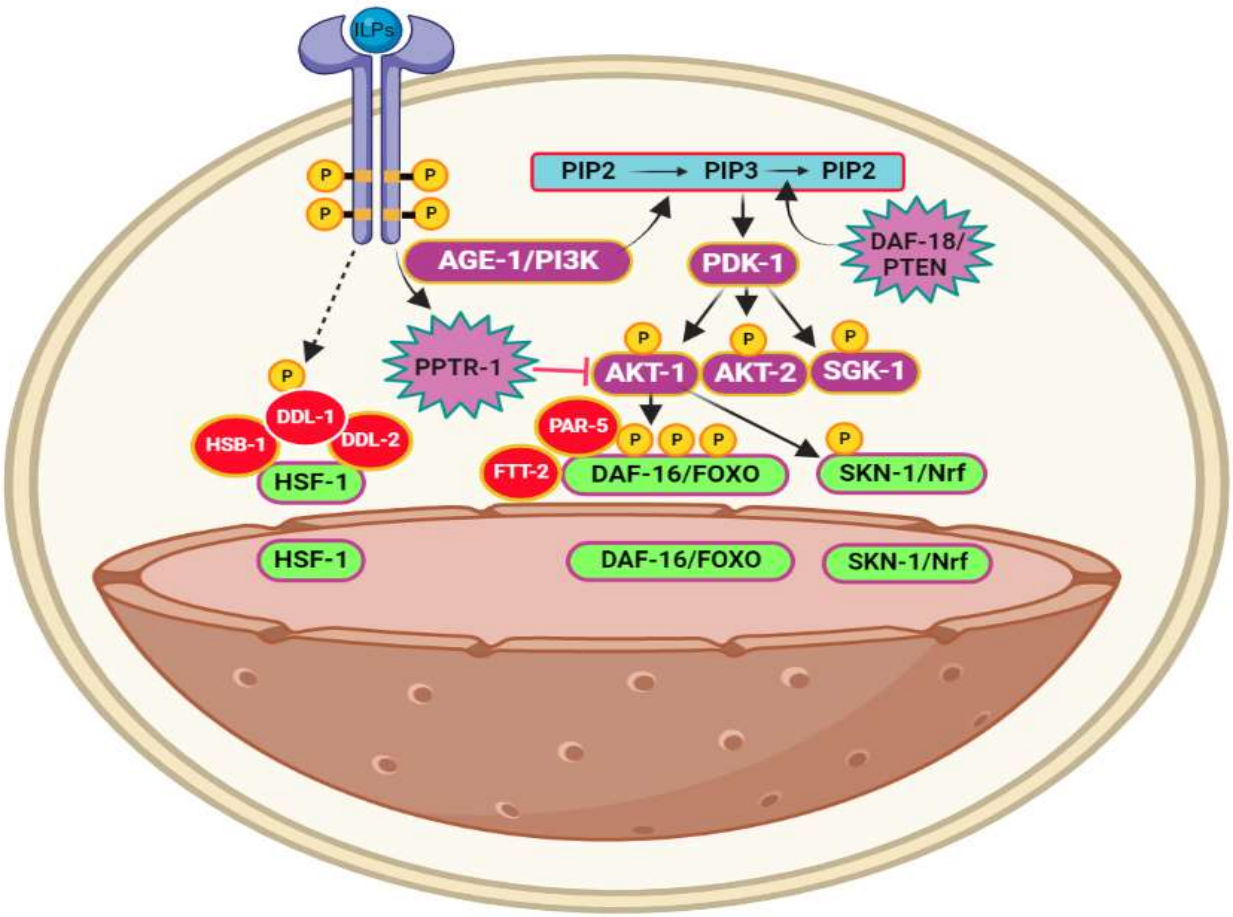

Figure 1. 2 The IIS/IGF-1 pathway

The insulin-like peptides (ILPs) bind to the DAF-2 transmembrane receptor resulting in its activation. Once DAF-2 is activated, it recruits and activates phosphoinositide 3 kinase (AGE-1/PIK3). As a result of this, the serine/threonine kinases (PDK-1, AKT-1, and AKT-2) are activated and result in the phosphorylation of the DAF-16/FOXO and SKN-1. PAR-5 and FTT-2 interact with phosphorylated DAF-16 to ensure its cytoplasmic retention. The DAF-18/PTEN lipid phosphatase and the serine/threonine phosphatase PPTR-1/PP2A counteract AGE-1/PI3K and AKT-1 signaling, respectively. On the other hand, HSF-1 is also retained in the cytoplasm after binding to the phosphorylated-DDL-1, DDL-2, and HSB-1 complex. The components that promote IIS are shown in purple, the ones that repress this pathway are shown in red and the transcription factors (DAF-16, SKN-1, and HSF-1) regulated by this pathway are colored green. Figure adapted and modified from Murphy and Hu, 2018 (42).

1.3.2 The MAPK Pathway:

Mitogen-activated protein kinases (MAPKs) are serine/threonine kinases that connect cell surface receptors to key regulatory targets within the cells (47). These enzymes are activated by various stimuli including growth factors, cytokines, stress signals, and neurotransmitters (48). The MAPK signaling cascades consist of three core kinases (MAPKKK, MAPKK, MAPK) with additional upstream (MAP4K) and downstream kinases (MAPKAPK). The sequential phosphorylation of kinases leads to the activation of regulatory targets by MAPK (49). The three most important MAPK signaling pathways are described below (Figure 1.3):

The ERK/MAPK pathway: In *C. elegans* , the ERK/MAPK pathway consists of LIN-45 (MAPKKK), MEK-2 (MAPKK), and MPK-1 (MAPK). This pathway is involved in diverse cellular processes such as hypodermal development, meiotic progression, protein degradation, and olfaction (32–34). An external growth factor (EGF) binds to the Receptor Tyrosine Kinase (RTK) resulting in its dimerization and autophosphorylation (53). The phosphorylated tyrosine residues serve as the binding site for adaptor proteins which then recruit the Guanine Exchange Factor (GEF) which, in turn, activates the small GTPase Ras (54). Ras-GTP binds LIN-45 (a *C. elegans* ortholog of mammalian RAF1), promoting its stable association with the plasma membrane. The scaffold protein KSR facilitates the activation of LIN-45 and recruits other components to promote this pathway (55). LIN-45 phosphorylates and activates MEK-2 (a *C. elegans* ortholog of mammalian MEK1/2) which further phosphorylates and activates MPK-1 (a *C. elegans* ortholog of mammalian ERK1/2) (56). Once MPK-1 is activated, it phosphorylates various transcription factors such as SKN-1. MPK-1 directly phosphorylates SKN-1 and results in its nuclear translocation. MPK-1 has been shown to be involved in the lifespan extension of *C. elegans*

through the phosphorylation and nuclear accumulation of SKN-1 (57). This pathway is also called the Raf-MEK-ERK pathway.

The c-Jun N-terminal Kinase (JNK) pathway: In *C. elegans* , the JNK pathway consists of JNK-1 (homolog of human JNK) and two MAPKK proteins MEK-1 and JKK-1. Both of these kinases, MEK-1 and JKK-1, serve as activators of JNK-1. This pathway has been shown to play a crucial role in coordinated motion in *C. elegans* . A mutation in *jkk-1* resulted in defective locomotion in worms which was rescued by the conditional expression of JKK-1 in adult mutants (58). In addition to coordinated locomotion, the JNK pathway is also involved in oxidative stress response and longevity. The *jnk-1* and *jkk-1* mutants show a significant reduction in lifespan suggesting that this pathway is involved in lifespan extension. JNK-1 must be phosphorylated by JKK-1 in order to induce longevity. Once JNK-1 is phosphorylated, it phosphorylates DAF-16 allowing its translocation to the nucleus where it regulates the transcription of its target genes thus conferring oxidative stress resistance and lifespan extension (59).

The p38 MAPK pathway: The p38 MAPK pathway plays an important role in adaptation, homeostasis, and specialized stress responses (60). This pathway is activated by diverse stimuli including oxidative stress. The oxidative stress inducers (sodium arsenite, *tert*-butyl hydroperoxide, and paraquat) result in the activation of the p38 MAPK pathway. This signaling cascade is composed of MAPKKK, SEK-1 (MAPKK), and PMK-1 (MAPK) (42). Under oxidative stress, SEK-1 phosphorylates PMK-1 which in turn phosphorylates SKN-1 at Ser-74 and Ser-340 residues leading to its nuclear localization where it activates the oxidative stress response genes such as *gcs-1* (42). This pathway has also been shown to be involved in providing innate immunity in *C. elegans* through NSY (MAPKKK), SEK-1 (MAPKK), and PMK-1 (MAPK) pathway (61).

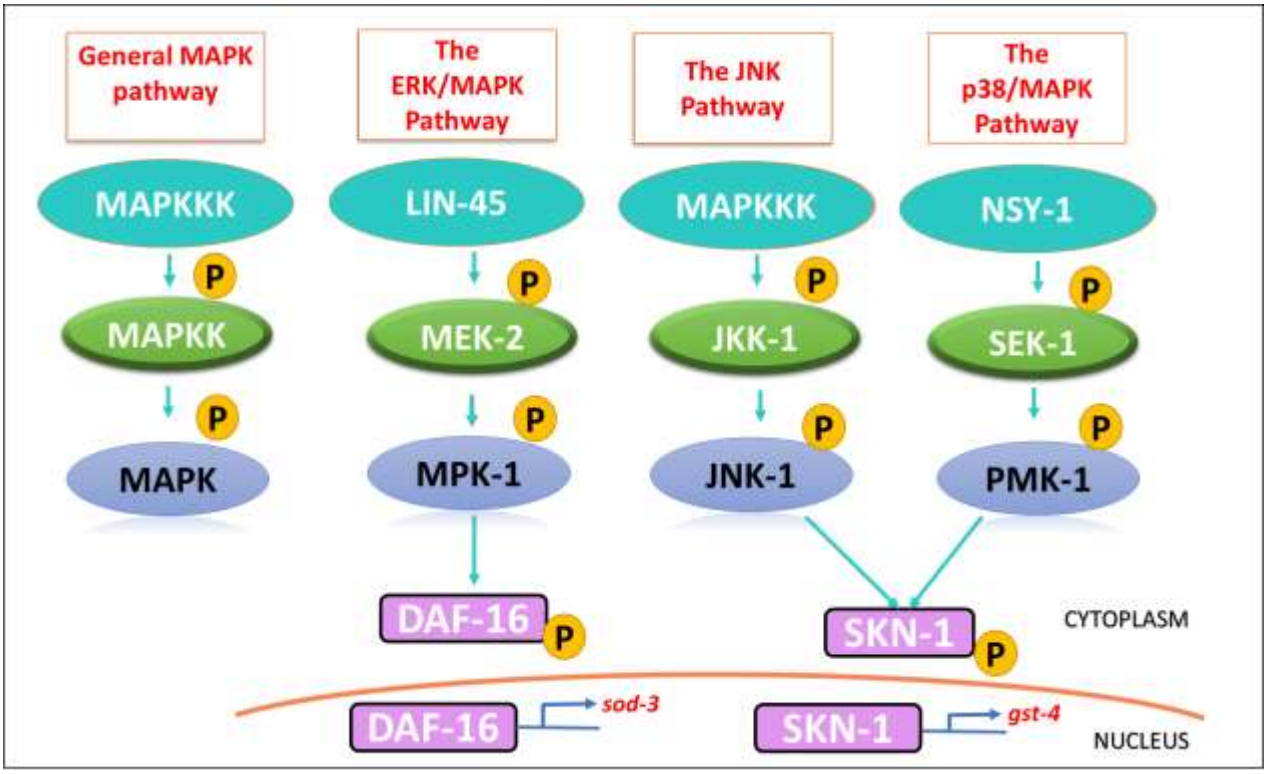

Figure 1. 3 The MAPK signaling pathway

The first cascade represents the general MAPK signaling pathway which consists of MAPKKK, MAPKK, and MAPK, each activating the next component via phosphorylation. The individual components of the ERK/MAPK, JNK, and the p38/MAPK pathways, in *C. elegans* , are shown opposite to the general MAPK pathway. The former pathway leads to the phosphorylation and activation of DAF-16 whereas the latter two pathways activate SKN-1 via phosphorylation. Respective components of the pathways were adapted from Okuyama *et al.*, 2010 (57), Oh *et al.*, 2005 (59) and Inoue *et al.*, 2005 (60).

1.4 Structure and Function of SKN-1:

In mammals, the Nrf/CNC family is composed of four closely related proteins Nrf1 (62), Nrf2 (63), Nrf3 (64), and p45 NF-E2 (65). Among these proteins, Nrf2 is mainly known for its role in defense against oxidative and xenobiotic stress (66). Under oxidative stress conditions, Nrf2 translocates to the nucleus, binds to antioxidant response elements (AREs), the upstream regulatory sequence of the target genes, and recruits the general transcription machinery of ARE-regulated genes (67). Under non-stressed conditions, Kelch ECH associating protein 1 (Keap1) retains Nrf2 in the cytoplasm and promotes its proteasomal degradation (68). Nrf2 uses the basic-region leucine zipper (bZIP motif), located on the C-terminus, to dimerize with small Maf proteins and other transcription factors allowing it to eventually bind DNA (69).

SKN-1 is the mammalian ortholog of Nrf2 and has diverged considerably from Nrf2 in regards to DNA binding, however, the functional similarity between Nrf2 and SKN-1 is remarkable (21). SKN-1 lacks the bZIP motif that Nrf2 requires for DNA binding but instead contains the helical structure in its C-terminus through which it recognizes bases in the DNA minor groove (70) (Figure 1.4A). In addition, it also contains a conserved region called the "DIDLID element" located between residues 99 and 112 of SKN-1 that is involved in transcription activation (71) and targeting SKN-1 for proteasomal degradation (72). In the mouse, rat, and human genomes, this region lies in the Neh2 domain of Nrf2 between amino acids 17 and 32 and is involved in the ubiquitination of Nrf2 and its rapid turnover during homeostatic conditions (73).

At least three protein isoforms of SKN-1 are found in *C. elegans* : SKN-1A, SKN-1B, and SKN-1C (74). SKN-1A is expressed in all tissues (57) whereas SKN-1B is expressed in two sensory neurons and SKN-1C is found only in the intestine (58-59). SKN-1A contains an N-terminal transmembrane domain (absent in SKN-1B and SKN-1C) that allows it to translocate to

the endoplasmic reticulum (77). Upon exposure to oxidative stress, SKN-1C localizes to cytoplasm suggesting that this form may be analogous to mammalian Nrf2 (78).

1.4.1 Regulation of SKN-1:

SKN-1 is regulated by many different pathways. The IIS transduction pathway is the negative regulator of SKN-1. Under normal conditions, AKT-1, AKT-2, and SGK-1 retain SKN-1 in the cytoplasm through phosphorylation [27]. On the other hand, the ERK/MAPK and p38/MAPK pathways serve as positive regulators of SKN-1. The phosphorylation of SKN-1 by MPK-1 and PMK-1 allows its translocation to the nucleus (42). Furthermore, WDR-23 and BRAP-2 serve as the negative regulators of SKN-1 (Figure 1.4B)

WDR-23 protein forms a complex with the damaged DNA binding protein 1 (DDB1), CUL4 (a ubiquitin ligase), and the proteasome to inhibit SKN-1-dependent transcription of phase II detoxification genes (79). Loss of WDR-23 results in elevated expression of SKN-1, significantly enhanced expression of phase II detoxification genes, worms with extended lifespans, and elevated resistance against oxidative stress (61).

Once SKN-1 is translocated into the intestinal nuclei, it promotes the transcription of phase I, II, and III detoxification proteins including Cytochrome P450, short-chain dehydrogenases (SDH), GSTs, UGT enzymes and ABC transporters (80,81).

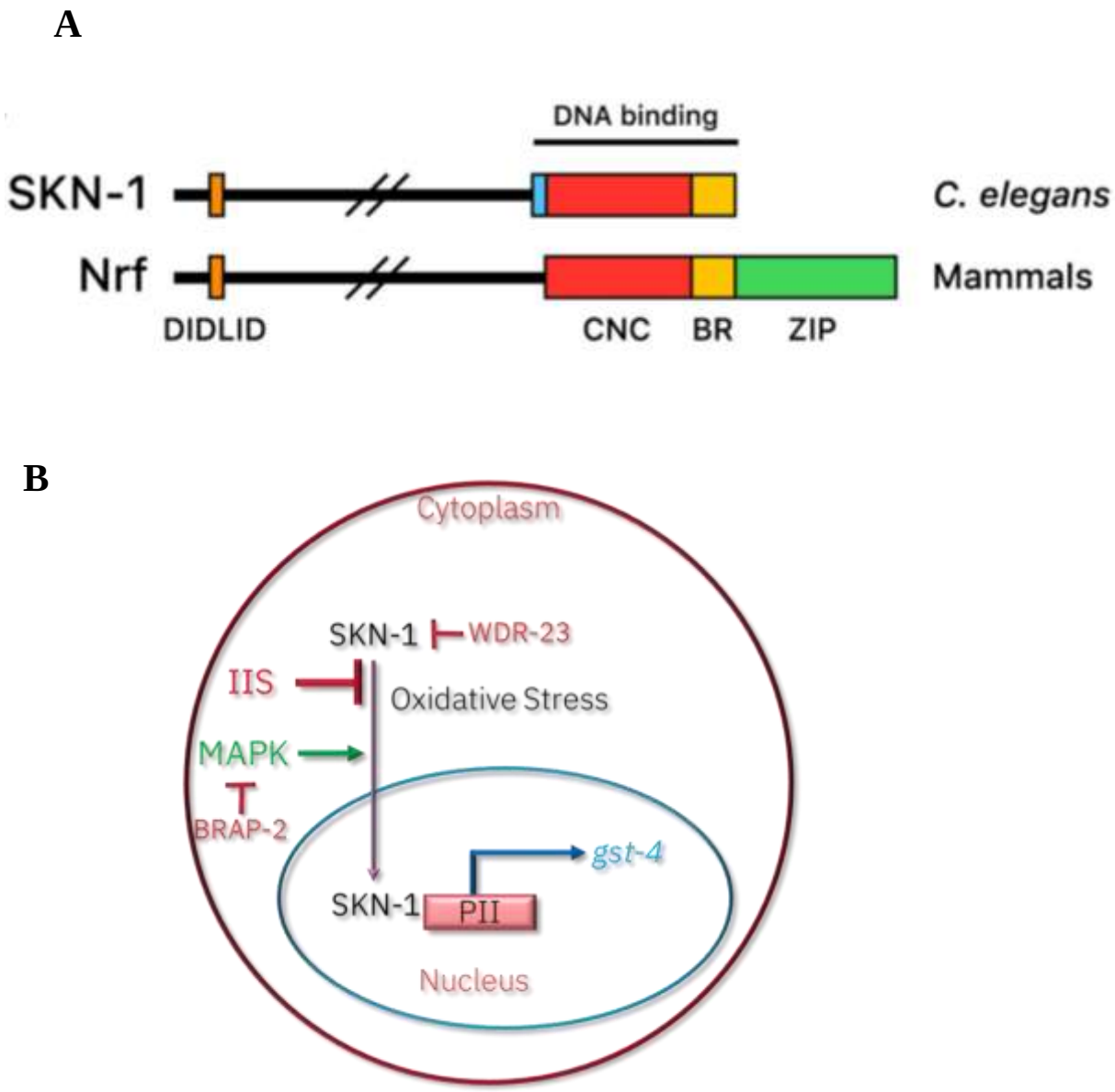

Figure 1. 4: Structure of SKN-1 in *C. elegans* compared to its mammalian orthologue Nrf and the regulation of SKN-1 by different factors.

(A) SKN-1 lacks the bZIP motif that is present in Nrf2, however, it contains the helical structure in its C-terminus through which it recognizes bases in the DNA minor groove. In addition, it also contains a conserved region called the "DIDLID element" that is involved in transcription activation and targeting SKN-1 for proteasomal degradation. Image adapted from Blackwell *et. el.*, 2015 (65). (B) SKN-1 is negatively regulated by the IIS pathway and WDR-23. However, it is positively regulated by the MAPK pathway. BRAP-2 also negatively regulates SKN-1 by inhibiting the MAPK pathway. Under oxidative stress conditions, the IIS is reduced, and BRAP-2 undergoes degradation ultimately resulting in the translocation of SKN-1 into the nucleus where it can induce the transcription of its target genes.

1.5 BRAP-2:

BRAP2 (BRCA-1 Associated Protein 2) is a cytoplasmic retention protein of BRCA1 where it binds to the nuclear localization signal (NLS) of BRCA1 and inhibits its translocation to the nucleus (82). BRAP2 also serves as a negative regulator of the Ras/MAPK pathway (Figure 1.5). Under the conditions when Ras is bound to GDP, BRAP2 binds to KSR and prevents it from recruiting the components of the Ras/MAPK pathway (83). However, when the Ras/MAPK signaling is triggered, Ras binds GTP and physically interacts with BRAP2. As a result of this, BRAP2 is ubiquitinated and autodegraded using its ubiquitin ligase activity (63). After BRAP2 is degraded, KSR is released and promotes the Ras/MAPK signaling cascade which will eventually result in the activation of MAPK which will phosphorylate the downstream target (84).

In *C. elegans* , BRAP2 is known as BRAP-2. Loss of *brap-2* renders worms highly sensitive to oxidative stress that can lead to early developmental arrest (85). In addition, BRAP-2 serves as a negative regulator of the p38/MAPK pathway. *brap-2* mutants show elevated expression of SKN-1-dependent, phase II detoxification genes that fall under the regulation of the p38/MAPK pathway (81). The removal of BRAP-2 results in enhanced expression of phase II detoxification genes that are activated by SKN-1 and ELT-3 interaction. In the absence of BRAP-2, PMK-1 phosphorylates SKN-1 and allows its localization to the nucleus where it physically interacts with ELT-3 and promotes the transcription of its target phase II detoxification genes (66).

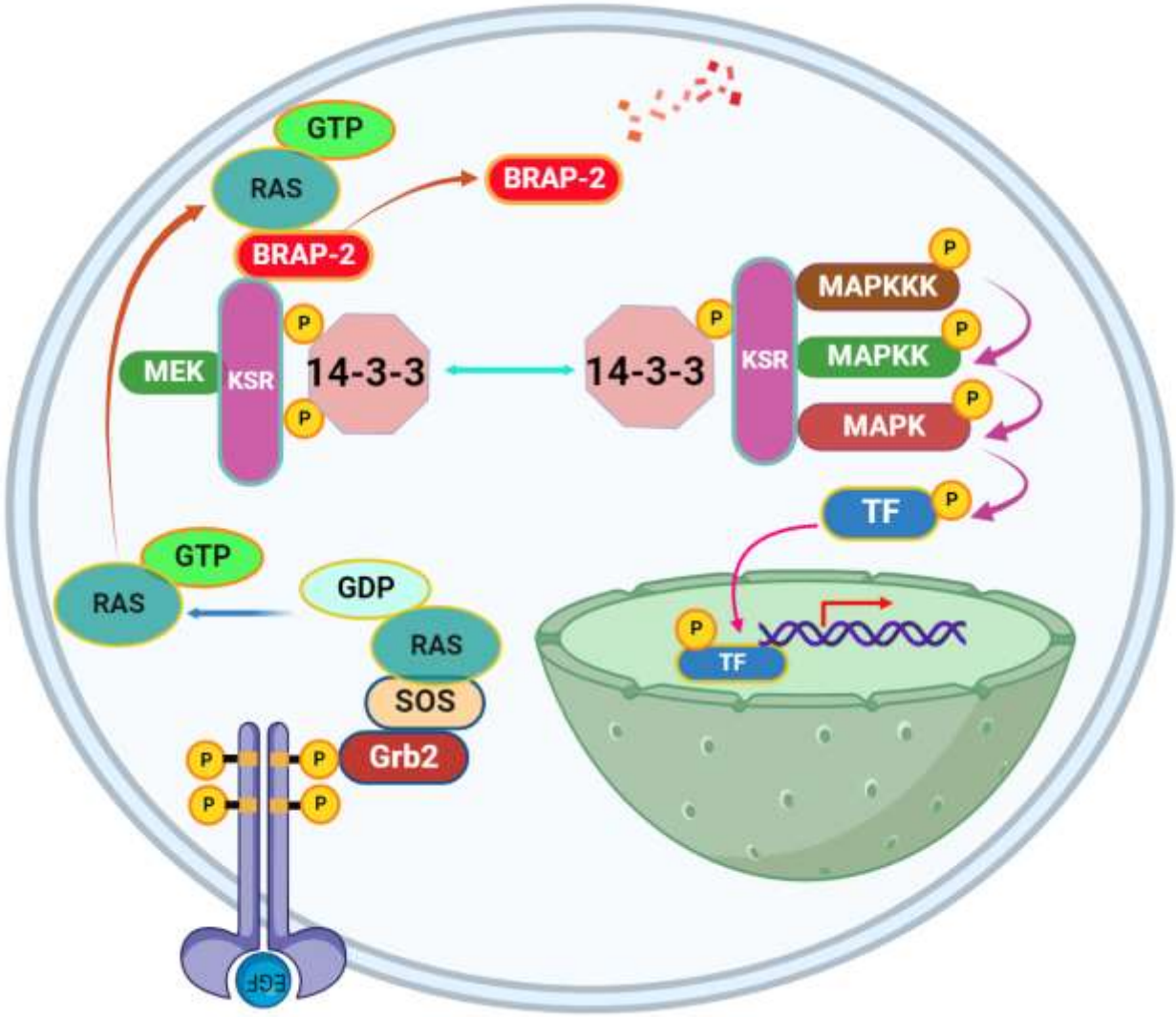

Figure 1. 5: BRAP2 serves as a negative inhibitor of the MAPK signaling pathway

Under normal conditions, BRAP2 binds KSR and prevents it from recruiting components of the MAPK pathway. However, when an extracellular growth factor (EGF) binds to the transmembrane receptor, RAS becomes active by binding to GTP. The RAS-GTP complex physically interacts with BRAP2 and triggers its autodegradation through its ubiquitin ligase activity. Once BRAP2 is autodegraded, KSR is released and promotes the MAPK signaling pathway by recruiting its components which eventually results in the phosphorylation and nuclear translocation of the target transcription factor. Adapted and modified from Kolch, 2015 (86).

1.6 DAF-16:

FOXOs belong to the O class of Forkhead box class transcription factors that are involved in a variety of cellular processes including cell cycle arrest, apoptosis, metabolism, stress resistance, and longevity (87). In mammals, there are four FOXO proteins; FOXO1, FOXO3, FOXO4, and FOXO6 whereas in invertebrates there is only one FOXO protein called DAF-16 (DAuer Formation-16), which is found in *C. elegans* (88).

When *C. elegans* experience unfavorable growth conditions (e.g., food deprivation, high temperature, overcrowding) during the early larval stage (L1), they can enter an alternative development mode called the "dauer stage" where they do not age or feed and survive for four to eight times longer than the wildtype worms (89). *daf-16* was initially isolated as a gene that caused dauer formation when mutated (90). Current research about DAF-16 reveals that it is regulated by a number of different signaling pathways and is not only involved in dauer formation but also regulates lifespan, metabolism, and stress response (91).

1.6.1 Regulation of DAF-16:

The IIS pathway, germline signaling and TOR signaling pathways serve as the negative regulator of DAF-16 (Figure 1.6). In the IIS pathway, AKT-1, AKT-2, and SGK-1 phosphorylate DAF-16 and sequester it in the cytoplasm (73,74). The worms with germline ablation live 60% longer than wild-type worms and this lifespan extension is dependent on DAF-16 (94). *daf-2* mutants live twice as long as N2 worms, however, when germline was ablated in *daf-2* mutants, their lifespan increased dramatically. Germline-ablated *daf-2* mutants live 4 times longer than wild-type worms (78). It is possible that signals from the reproductive system and IIS pathway integrate to regulate DAF-16. In addition, the TORC1 complex (part of the mTOR signaling pathway) negatively regulates DAF-16 as well as SKN-1. The inhibition of TORC1 results in

enhanced expression of SKN-1 and DAF-16 target genes (95). However, lifespan extension resulting from the inhibition of TORC2 (another component of the mTOR signaling pathway) is dependent on SKN-1 and not DAF-16 [76].

On the other hand, the JNK pathway and the AMPK pathway serve as the positive regulators of DAF-16. JNK-1 physically interacts with DAF-16, on sites that are different from where AKT binds DAF-16, and phosphorylates it to allow its translocation to the nucleus (59). The AMPK pathway also acts as a positive regulator of DAF-16 where AAKG-4 phosphorylates DAF-16 and allows its nuclear localization. Once in the nucleus, DAF-16 triggers the transcription of genes that activate AAKG-4 thus forming a positive feedback loop (96). *daf-2* mutants show higher expression of AAKG-4 which can be linked to the interaction between DAF-16 and AAKG-4 existing through a positive feedback mechanism (77).

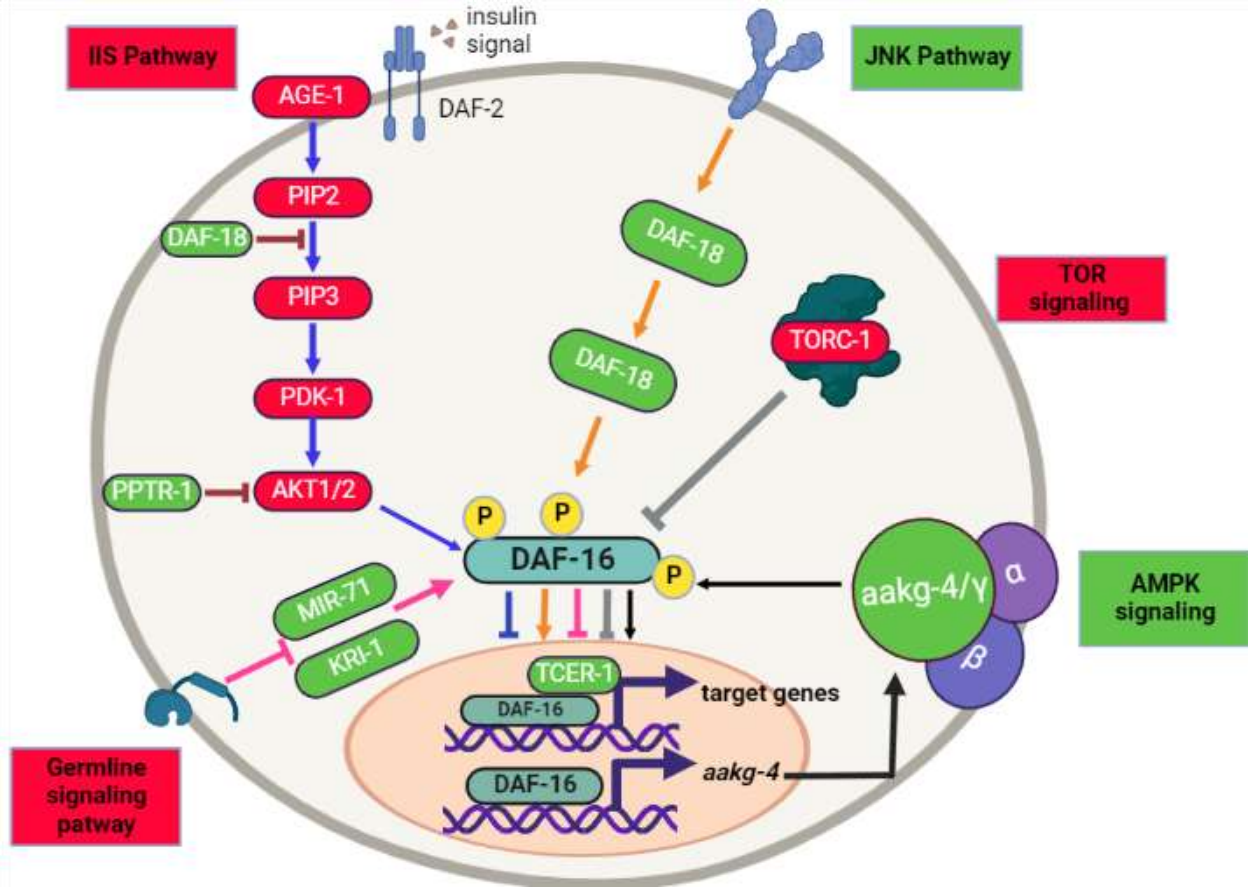

Figure 1. 6: Regulation of DAF-16/FOXO

Multiple signaling pathways regulate the function of DAF-16/FOXO by either sequestering it in the cytoplasm or promoting its translocation to the nucleus. IIS, TOR and Germline signaling pathways are inhibitors of DAF-16 whereas AMPK and JNK pathways serve as positive regulators. The negative regulators are shown in pink and the positive regulators are shown in green. Each pathway is represented by a specific-colored arrow. Image adapted and modified from Sun *et al*., 2017(97).

1.7 Literature review of ZTF-22:

The *C. elegans* ZTF-22 belongs to the zinc-finger family of transcription factors. Zinc finger proteins (ZFPs) are named so because a short region of amino acid residues folds around a zinc atom in the shape of a finger (98). These proteins are prominent for their role in the recognition of DNA (78), but they have also been found to function in RNA binding (99) and participating in protein-protein interactions (100). ZTF-22 is located on chromosome II and is a $Cysteine_2/Histidine_2$ (C_2H_2) type of zinc finger transcription factor (Wormbase). In C_2H_2 transcription factors, two histidine residues on the α-helix and two cysteine residues on the β-sheet interact with the zinc atom (Figure 1.7A). The C-terminal of the finger contains the α-helix whereas the N-terminal contains the β-sheet, and the zinc fingers form a loop around DNA in such a fashion that the α-helices of each finger directly contact the DNA (98). According to Wormbase (an online database containing information about the biology and genome of *C. elegans*), two isoforms of this gene exist. Isoform a is 448 aa in length whereas the isoform b is 449 aa long.

In this project, the wild-type *C. elegans* strain, N2, and the *ztf-22* mutant strain, *ztf-22(gk3296),* were used. The *ztf-22* mRNA in the N2 strain is composed of five exons whereas the *ztf-22* mRNA in the *ztf-22(gk3296)* strain contains a deletion mutation in the first half of the third exon (Figure 1.7B). The impact of this mutation on the protein structure of ZTF-22 is currently unknown.

In *vivo* analysis showed that *ztf-22* transcripts were enriched near the TRA-1 binding site. TRA-1 is a zinc finger transcription factor that plays an important role in sex determination in *C. elegans* where it promotes female development by repressing male-specific genes (101). Based on this study, it is not far-fetched to assume that ZTF-22 may be working with TRA-1 to mediate sex determination in *C. elegans* .

Based on overall ontology, ZTF-22 is expressed in the dorsal nerve cord, head muscle, head neurons, intestine, and ventral nerve cord (Wormbase). While based on its protein structure, some characteristics of ZTF-22 have been described, however, its general biological role and its function specifically in response to oxidative stress remain unknown. Using *C. elegans* as a model organism, I have attempted to understand the function of ZTF-22 in response to oxidative stress and its general biological role in terms of longevity and response to various stressors.

A

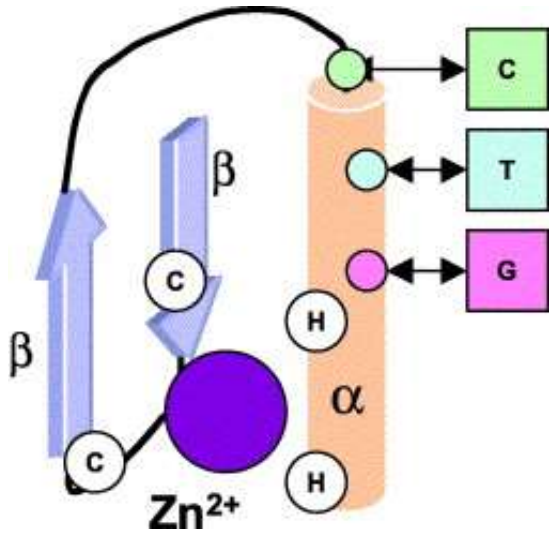

B

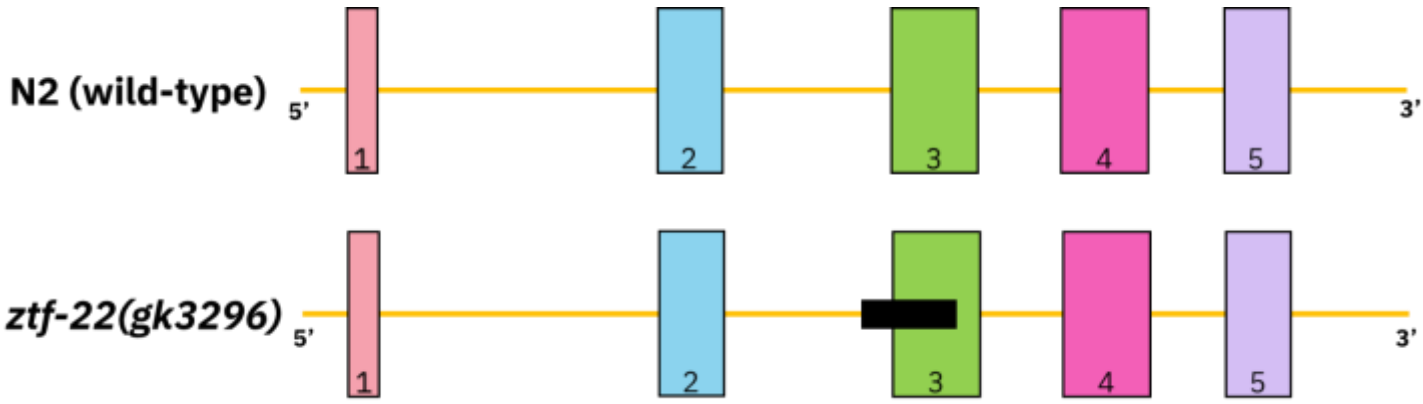

Figure 1. 7: Structure of a generic C_2H_2 type of zinc-finger transcription factor and comparison between the structures of *ztf-22* mRNA in N2 and *ztf-22(gk3296)* worms.

(A) The general structure of a C_2H_2 zinc-finger motif. It is composed of ββ-α fold where amino acid residues in the α-helix recognize and bind to specific sequences in the target DNA molecule. Image adapted from Uil *et al*., 2003 (103). (B) The comparison of the *ztf-22* mRNA structure between N2 and *ztf-22(gk3296)* strains. The *ztf-22* mRNA is composed of five exons in N2 worms whereas in the *ztf-22(gk3296)* strain, a deletion mutation is present in the first half of the third exon in *ztf-22* mRNA.

1.8 Rationale, Hypothesis, and Objectives of this Thesis:

Previously, our lab carried out a transcription factor-specific RNAi screen on *brap-2* mutants using a *C. elegans* strain that contained a GFP coding region fused to the *gst-4* promoter (*gst-4p::gfp*). This was done to monitor for changes in *gst-4* expression. We found that RNAi knockdown of *ztf-22* and *ztf-17* resulted in an increase in GFP expression, similar to what is seen with *brap-2* and *wdr-23* knockdowns. Further research on ZTF-17 by a member of our lab, revealed that ZTF-17 acts as a repressor of PI (*sod-3, ctl-1/2, ins-7, mtl-1/2, dod-3 and dod-17)* and PII genes (*gst-4* and *gcs-1*). *ztf-17* also provides short-term resistance to oxidative stress against sodium arsenite but renders worms highly sensitive to heat stress. It is possible that ZTF-17 and ZTF-22 may be working together in a complex to regulate the expression of *gst-4.*

Based on this initial RNAi screen, my hypothesis is that ZTF-22 has a role in attenuating the expression of PII detoxification enzymes. Thus, the main objective of this research is to understand the role of ZTF-22 in oxidative stress response in *C. elegans* and its effect on *gst-4* expression using molecular and genetic techniques. My additional objectives are to determine whether (1) *ztf-22* is required for survival under oxidative stress induced by sodium arsenite (As) and *tert*-butyl hydroperoxide (tBOOH), (2) *ztf-22* is required for survival under ER stress induced by Dithiothreitol (DTT), (3) *ztf-22* causes lifespan extension in *ztf-22* mutants and (4) *ztf-22* is required to protect against thermotolerance. Thus, the main objective of this thesis is to characterize the role of ZTF-22 in oxidative stress response, especially the PII detoxification genes, and determine its role in longevity.

CHAPTER 2: MATERIALS AND METHODS

2. Materials and Methods:

2.1 The maintenance and genetics of *C. elegans* strains:

All the *C. elegans* strains used in this project were obtained from the *Caenorhabditis* Genetics Center (The University of Minnesota) and the National Bioresource Project (Tokyo, Japan). The strains were maintained under standard conditions according to the protocol designed by Sydney Brenner (104). All experiments were performed using N2 as the wild type at a temperature of 20 degrees Celsius unless specified otherwise. The following strains of *C. elegans* were used in this study: YF215 [*ztf-22(gk3296)II*], DR466 [(*him-5(e1490)V]*, CL2166 [*dvIs19(gst-4p::gfp)III]*, YF220 [*ztf-22(gk3296)II; dvIs19(gst-4p::gfp)III*], CF1553[*muls84(sod-3p::gfp)*], and YF224 [*ztf-22(gk3296)II; muls84(sod-3p::gfp)*].

2.2 Generation of transgenic worms:

The backcrossed YF215 [*ztf-22(gk3296)*] strain was used to generate two types of transgenic worm strains: YF220 [*ztf-22(gk3296)II; dvIs19(gst-4p::gfp)III*] and YF224 [*ztf-22(gk3296)II; muls84(sod-3p::gfp)*].

In order to generate *ztf-22(gk3296); dvIs19(gst-4p::gfp)* transgenic worms, male mutant worms, *him-5(e1490)*, were crossed with *dvIs19(gst-4p::gfp)* hermaphrodites at L4 stage. As a result of this cross, green male worms expressing *dvIs19(gst-4p::gfp)* were collected, using the florescent microscope, and crossed with *ztf-22(gk3296).* These worms were considered Parental worms or P1. The green hermaphrodites produced as a result of this cross were considered F1. Individual F1 worms were allowed to lay eggs to produce F2 progeny. The worms from F2 were transferred to separate NGM plates where they were allowed to reach the L4 stage and lay eggs (F3). Single Worm PCR (SW-PCR) was performed to determine the genotype of these F2 worms. Once, the plate containing worms with *ztf-22(gk3296)* deletion was found, SW-PCR is performed

again to ensure that all the worms on this plate were homozygous for *ztf-22(gk3296)* mutation and expressed *dvIs19(gst-4p::gfp).*

To generate *ztf-22(gk3296); muls84(sod-3p::gfp)* transgenic worms, male mutant worms, *him-5(e1490),* were crossed with *muls84(sod-3p::gfp)* hermaphrodites at L4 stage. As a result of this cross, green male worms expressing *muls84(sod-3p::gfp)* were collected, using the florescent microscope, and crossed with *ztf-22(gk3296).* These worms were considered Parental worms or P1. The green hermaphrodites produced as a result of this cross were considered F1. Individual F1 worms were allowed to lay eggs to produce F2 progeny. The worms from F2 were transferred to separate NGM plates where they were allowed to reach the L4 stage and lay eggs (F3). SW-PCR was performed to determine the genotype of these F2 worms. Once, the plate containing worms with *ztf-22(gk3296)* deletion was found, SW-PCR was performed again to ensure that all the worms on this plate were homozygous for *ztf-22(gk3296)* mutation and expressed *muls84(sod-3p::gfp).*

2.3 Single Worm – Polymerase Chain Reaction:

A single worm was placed in the 20µl PCR tube containing 4µl of Single Worm Lysis buffer. The Single Worm Lysis buffer was prepared by mixing 10x thermopol buffer (NEB E50000S), Proteinase K (NEB P8107S), and sterile filtered water. The tube was stored at -80 ^{o}C. The next day, the tube was heated in the thermocycler at 65 ^{o}C for 1 hour. To inactivate proteinase K, the tube was incubated at 95 ^{o}C for 15 minutes. The tube was removed from the thermocycler (Biometra T Personal Thermocycler) and 20 µl of PCR master mix was added to it. The PCR master mix was prepared by mixing 20 µl of 10x thermopol buffer (NEB E50000S), 20 µl of 2mM dNTP (NEB E50000S), 1 µl of 100 µM forward primer, 1 µl of 100µM reverse primer, 1 µl of Taq polymerase (NEB E50000S) and 157 µl of nuclease-free H_2O (Bioshop WAT222). The

reaction mixture was then placed in the thermocycler with melting and annealing temperatures corresponding to the forward and reverse primers used in the reaction. The product obtained as a result was verified by gel electrophoresis and the bands were observed using UV light (Alphaimager). The 1% agarose gel used to perform gel electrophoresis was prepared by mixing 50 ml of TAE (Thermofisher B49) buffer with 0.5g of Agarose (Sigma A9539-50G).

2.4 Worm Synchronization:

A few healthy L4 staged worms (12-15) were placed on NGM plates seeded with OP-50 (*E. coli* bacterial food source). These worms were allowed to lay eggs for 4-5 hours, after which they were returned to their original plate and the eggs were maintained for 48 hours under standard conditions. After 48 hours, the eggs had hatched, and the worms had reached the L4 stage. These synchronized worms were used for further experiments.

2.5 RNA extraction and quantitative Real-Time PCR:

Before RNA extraction, synchronized worms were collected by washing the 6cm plate with 1.5 mL of M9 buffer, and the mix was transferred to a microfuge tube. The tube was centrifuged at 1000 x g for 30 seconds. The supernatant was aspirated and 1 mL M9 buffer was added to the tube after which it was centrifuged again. This step was repeated three times. After the final wash, the supernatant was removed, and the remaining worm pellet (~200 µl) was stored overnight at -80 ^{o}C. For RNA extraction, the microfuge tube was thawed and 250 µl of TRI reagent (Sigma 93289) was added to it. The tube was then placed on a vortex shaker at 4 ^{o}C for 15 minutes. After the 15 minutes had lapsed, 250 µl of absolute ethanol was added to the tube and it was vortexed briefly. The content of the tube was transferred to the Zymo-spin IC column (Zymo R2060) and the process of RNA extraction was carried out by following the manufacturer's protocol. Fisher Thermo NanoDrop 2000 was used to measure the total RNA concentration. The RNA sample was

used to synthesize cDNA by using the OneScript® Plus cDNA synthesis kit according to the manufacturer's protocol. The mRNA expression levels of various genes were measured by qRT-PCR by using specific primers and either BrightGreen 2X qPCR MasterMix (abm MasterMix-S) or BlasTaq™ 2X qPCR MasterMix (abm G891) and the Qiagen Rotor-gene Q system. The data were analyzed by the ΔΔCT method using measurements obtained from three independent trials. The mRNA expression levels of the experimental strain were normalized to the wildtype (N2) strain. *tba-1* and *cdc-42* were used as endogenous control genes unless specified otherwise.

2.6 RNA interference:

For RNA interference (RNAi), the transcription factor RNAi library, generated by Walhout lab, was used. The recipe for the NGM plates was slightly modified to perform RNAi. The following ingredients were added to agar before it was poured into plates; 0.4 mM IPTG, 100 µg/mL Ampicillin and 12.5 µg/mL Tetracycline. The plates were seeded by HT115 *E coli* expressing either the pL4440 control bacterial plasmid or dsRNA homologous to the target gene cloned into pL4440. Worms were allowed to reach the L4 stage on RNAi plates before they were observed under the confocal microscope for GFP quantification.

2.7 Fluorescence Microscopy and GFP quantification:

Two percent agarose pads were secured on microscope slides. A drop of 2mM levamisole solution was added to the agarose pad. Live L4 worms were suspended in the levamisole solution, and the slide was covered by a coverslip. Anesthetized worms were observed under the Zeiss Observer Z1 Spinning Disk Confocal Microscope. Images were captured using the tile scan and Z-stack features of the microscope and analyzed using ZEN 2.6 Software®. ImageJ software was used to quantify whole worm fluorescence.

2.8 Longevity Assay:

The L4 N2 and *ztf-22* mutant worms were allowed to lay eggs for 4-5 hours, after which they were transferred back to their original plates. The eggs were followed over time to see which strain lived longer. The worms were regularly transferred to fresh plates to prevent contamination, crowding, and starvation and provide a fresh supply of food. The worms that had crawled to the walls of the plate and desiccated or exploded or lost were not included in the total sample size. Three independent trials were performed.

2.9 Oxidative Stress Assays:

Two types of reagents were used to perform oxidative stress assays according to the protocol developed by Edwald *et al.* (2017): sodium arsenite (As) and *tert*-butyl hydrogen peroxide (*t*BHP).

For the sodium arsenite assay, L4 N2 worms and *ztf-22(gk3296)* mutants were placed in 500 µl of 5 mM As (as the experimental group) and 500 µl of M9 buffer (as the control group). Worms were counted every hour, the worms that did not respond to prodding by worm pick were considered dead. For analysis, data were collected from three independent experiments, conducted in triplicates.

For the tBHP assay, 7.5 mM *t*BHP plates were prepared one day before the experiment. Twelve L4 N2 worms and *ztf-22(gk3296)* mutants were placed on unseeded *t*BHP plates (experimental group) and regular unseeded NGM plates (control group). In the first 2 hours, worms that strayed from the center were constantly brought back to the center to keep them from drying on the wall of the plate. Worms were counted every hour and the ones that did not respond to prodding were considered dead. For analysis, data were collected from three independent trials, conducted in triplicates.

2.10 Thermotolerance Assay

For the thermotolerance assay, L4 N2 and *ztf-22(gk3296)* mutants were placed on NGM plates. The plates were placed in 37 ^{O}C incubator. The worms were counted every hour and the ones that did not respond to gentle probing by the wormpick were assumed dead. For control group, both strains were placed on NGM plates at 20 ^{O}C. For analysis, data were collected from three independent trials, conducted in triplicates.

2.11 ER stress Assay:

For the endoplasmic reticulum (ER) stress assay, 10 mM Dithiothreitol (DTT) plates were prepared one day before the experiment. L4 N2 and *ztf-22(gk3296)* mutant worms were placed on DTT plates. NGM plates that did not contain DTT served as control plates for both strains. Worms were scored every hour for survival. Animals that were unresponsive to repeated poking were considered dead. For analysis, data were collected from three independent trials, conducted in triplicates. Fresh plates were prepared before each trial.

2.12 Primer design:

Primer3 and BLAST (NCBI) programs were used to design primers used in this project. Primer pairs were selected based on the parameters of GC%, optimal Tm, and self-complementarity. Primers TK319 and TK320 were used to genotype *ztf-22(gk3296)* deletion mutants.

2.13 Statistical Analysis:

GraphPad Prism 8 Software was utilized to generate graphs and analyze data. Statistical methods, Multiple *t*-tests or Two-tailed Unpaired Student's *t*-test were used to establish statistical significance. Log-rank (Mantel-Cox) method was used to calculate the statistical significance of

survival and longevity assays. Data showing p values below 0.05 were considered statistically significant. Error bars represent the +/- standard error of the mean.

CHAPTER 3: RESULTS

3.0 Results:

3.1 knockdown of *ztf-22* by RNAi enhances *gst-4* expression (RNAi and qRT-PCR)

Previously, our lab carried out a transcription factor specific RNAi screen using a *C. elegans* strain that contained GFP coding region fused to the *gst-4* promoter (*gst-4p::gfp*) to monitor for changes in *gst-4* expression. This screen revealed that knockdown of *ztf-22* resulted in an enhanced expression of *gst-4* suggesting it may potentially be a negative regulator of *gst-4.* To corroborate this result, a *ztf-22* mutant strain, *ztf-22(gk3296)* was obtained from *Caenorhabditis* Genetics Center (CGC), and it was backcrossed with N2 to remove any background mutations. After the backcross, I generated transgenic worms carrying *ztf-22(gk3296)* deletion mutation along with *gst-4p::gfp* reporter construct (known as *ztf-22;gst-4p::gfp*) to visualize *gst-4* expression, under the confocal microscope. *ztf-22;gst-4p::gfp* worms appeared significantly brighter than the wild-type worms indicating stronger expression of *gst-4* in the mutants. Figure 3.1 (B,C) shows a 1.46x times higher *gst-4* expression in *ztf-22(gk3296)* worms compared to wild-type (*gst-4p::gfp*) worms. In addition to looking at *gst-4*, I was also curious about the impact of *ztf-22(gk3296)* mutation on the PI gene, *sod-3.* To achieve this, I generated *ztf-22(gk3296);sod-3p::gfp* transgenic worms which carried *ztf-22(gk3296)* mutation and expressed *sod-3* through GFP expression. These worms appeared 2.55 times brighter than the wild-type (*sod-3p::gfp*) worms when visualized under the confocal microscope indicating a noticeable increase in *sod-3* activity (Figure 3.1 B,D).

To further consolidate these results, mRNA levels of *gst-4* and *sod-3* were measured, in *ztf-22(gk3296)* mutants and N2 worms, using qRT-PCR. The qRT-PCR results were consistent with previous results showing comparatively higher expression of *gst-4* and *sod-3* in *ztf-22(gk3296)* mutants. The mRNA levels obtained from qPCR showed a 5-fold increase in *gst-4* and a 2.5-fold increase in *sod-3* expression in *ztf-22(gk3296)* mutants when normalized to the *tba-1*

reference gene (Figure 3.2 A). Whereas a 1.3-fold increase was observed in *gst-4* expression and a 2-fold increase in *sod-3* expression when the data was normalized to the *cdc-42* reference gene (Figure 3.2B). For the normalization of these qPCR data, two housekeeping genes (*tba-1* and *cdc-42*) were used. However, for the rest of the qPCR experiments, only *tba-1* was used to normalize the data as the CT values of *tba-1* were consistent more frequently than the *cdc-42*'s CT values. These results were obtained from 3 independent experiments. Taken together, these results suggest that ZTF-22 functions to repress the expression of oxidative stress resistance genes, *gst-4* and *sod-3*.

A

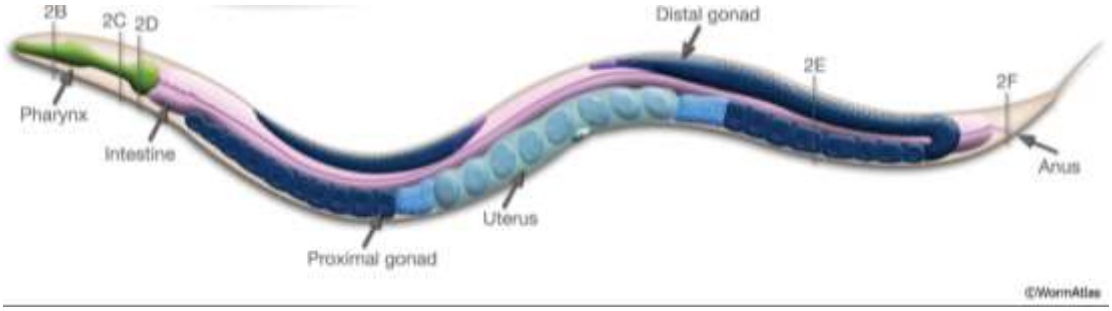
2B
2C
2D
Distal gonad
2E
2F
Pharynx
Intestine
Anus
Uterus
Proximal gonad
©WormAtlas

B

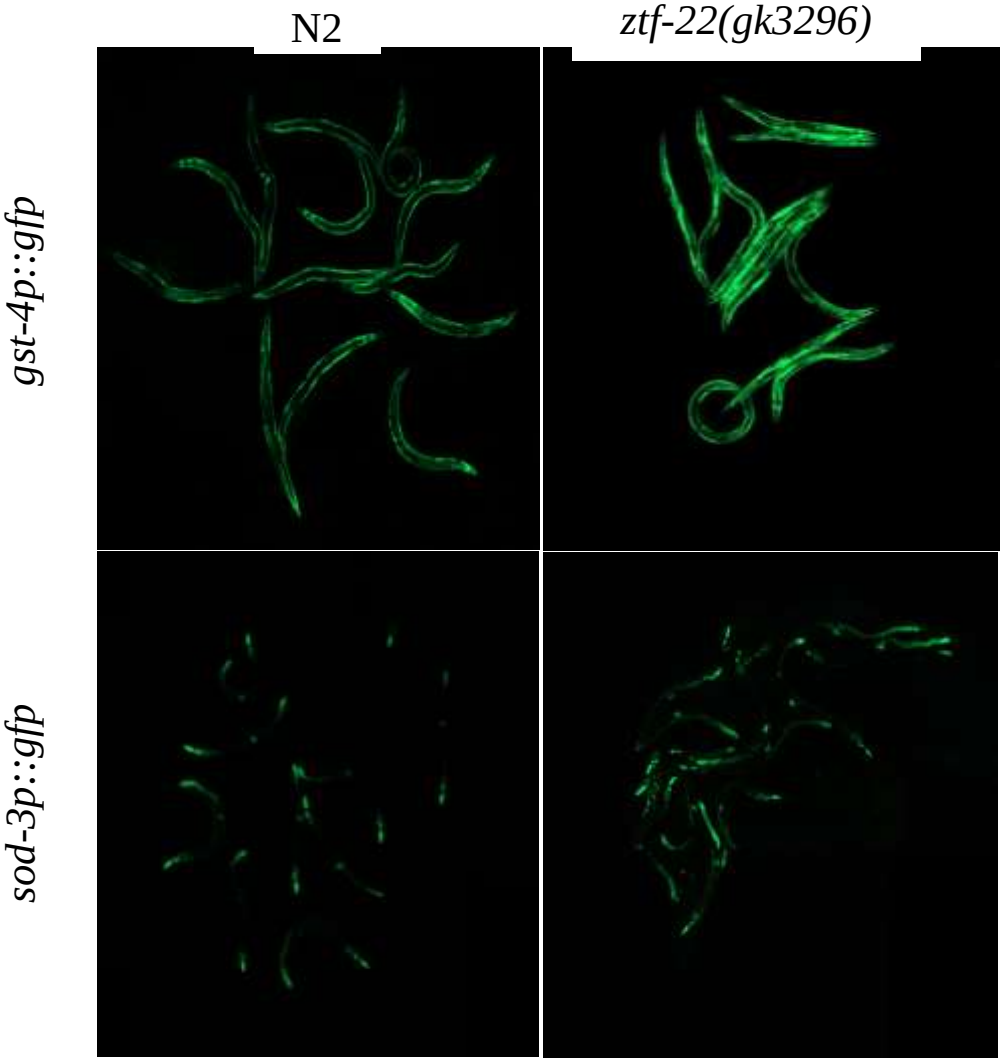
N2
ztf-22(gk3296)
gst-4p::gfp
sod-3p::gfp

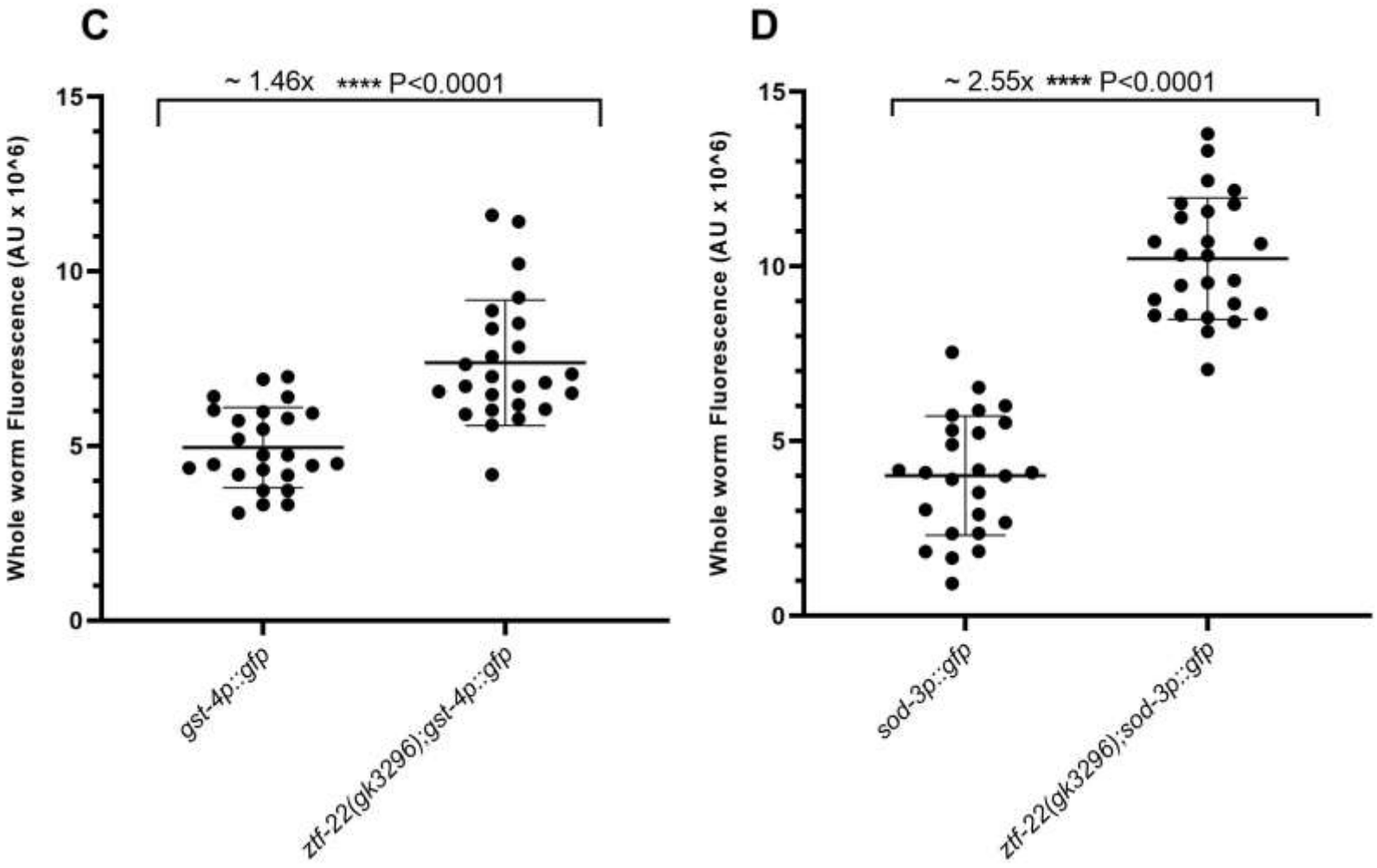

Figure 3.1: *ztf-22(gk3296)* mutants show higher expression of *gst-4* and *sod-3* genes compared to N2 worms.

(A) Anatomy of *C. elegans* , image was obtained from WormAtlas (105). (B) Whole worm fluorescence was visualized in transgenic worms with *ztf-22(gk3296)* mutation. The worms were viewed, and the images were captured using the confocal microscope under 10X magnification. (C-D) Fluorescence intensity was quantified using ImageJ Software. Results for n=25 worms are shown as individual points as the difference between the intensity readings per worm minus the background fluorescence. The solid black line represents the mean fluorescence intensity for each worm strain. GFP levels of *gst-4p;ztf-22(gk3296)* mutants were ~ 1.46x brighter than *gst-4p*::*gfp* whereas *ztf-22;sod-3::gfp* worms were 2.55x brighter than *sod-3p*::*gfp* worms. Statistical analyses were performed using the Two-tailed Unpaired Student's t-test; *** $P < 0.001$.

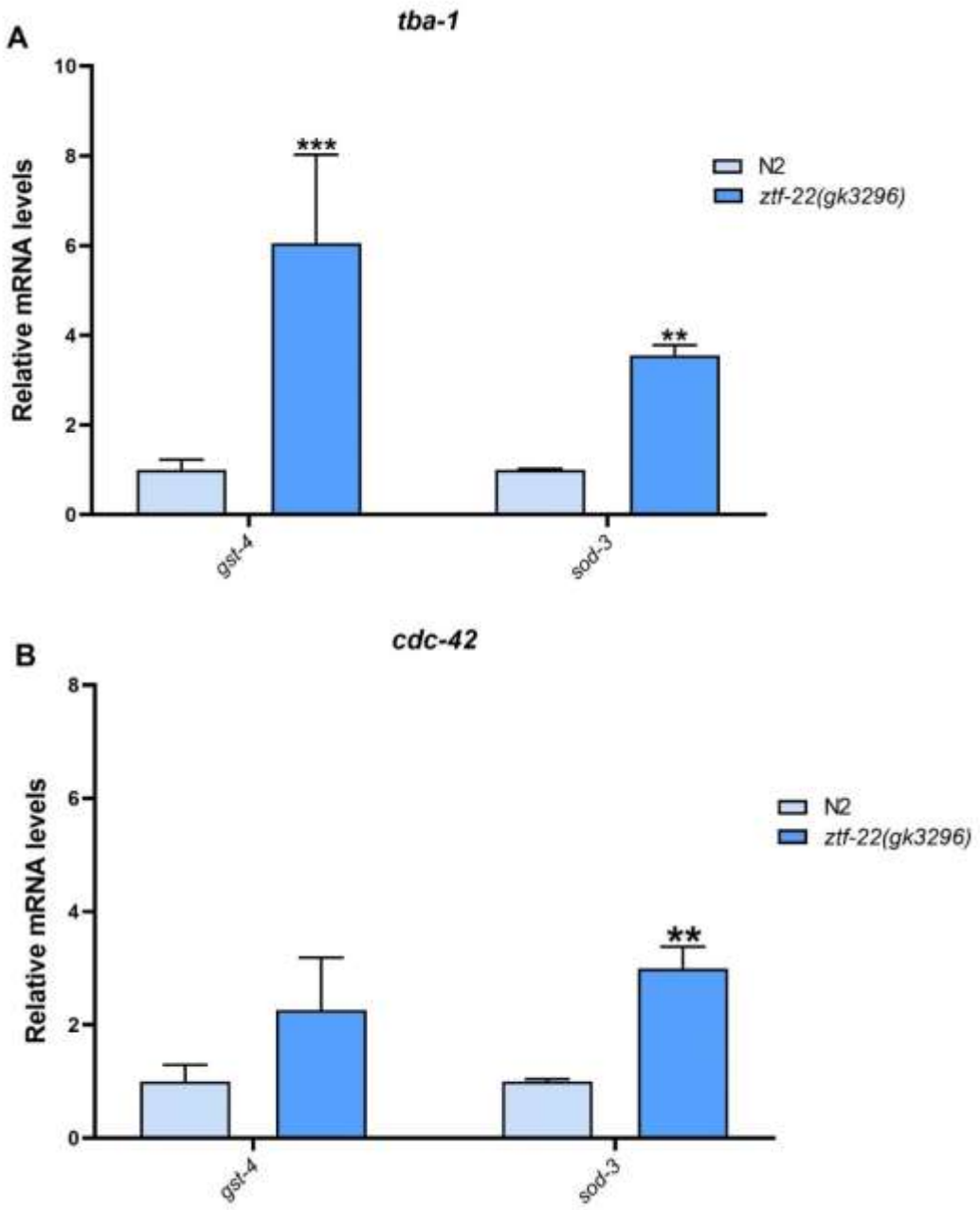

Figure 3.2: *ztf-22(gk3296)* mutants show elevated expression of *gst-4* and *sod-3*

The relative mRNA levels of phase I (*sod-3)* and phase II (*gst-4*) detoxification genes in wild-type (N2) and *ztf-22* mutant worms were determined using qPCR. Relative mRNA levels were normalized to *tba-1*(A) and *cdc-42* (B) reference genes. Results were obtained from three independent trials. Statistical analysis was carried out using Multiple *t*-tests. Error bars represent ± SEM; *** $P < 0.001$, ** $P < 0.01$.

3.2 ZTF-22 attenuates expression of phase I and II detoxification genes (qRT-PCR)

After learning that ZTF-22 negatively regulates *gst-4* and *sod-3* expression through transgenesis and qRT-PCR, I was curious to know whether this protein influenced the expression of other PII and non-phase II genes. I used qRT-PCR to measure the mRNA levels of some PII (*ugt-13, gsto-2, dhs-8, sdz-8,* and *gcs-1*) and non-phase II (*sod-1, sod-2, hsp-4,* and *fmo-2*) genes. The purpose of this experiment was to learn whether ZTF-22 has a general effect on detoxification genes. The results obtained from this experiment were analyzed using GraphPad Prism 8 and compared to N2. The housekeeping gene, *tba-1,* was used to normalize the data.

Among phase II genes, *ugt-13* showed decreased expression whereas *gsto-2* showed 2-fold increased expression in *ztf-22(gk3296)* mutants. However, no change was observed in the expression levels of *dhs-8, sdz-8,* and *gcs-1* (Figure 3.3A). From non-phase II genes, *fmo-2* showed decreased expression (Figure 3.3B). I decided to test the mRNA levels of other genes from the *fmo* family *(fmo-1, fmo-3, fmo-4, and fmo-5)* . The mRNA levels of *fmo-1, fmo-4,* and *fmo-5* were declined with *ztf-22* mutation (Figure 3.4A). Since *fmo-2*'s expression is influenced by *hif-1, nhr-49,* and *mdt-15,* I tested their mRNA levels to see whether ZTF-22 regulated the expression of *fmo-2* through these genes (Figure 3.4B). All of these genes showed reduced mRNA expression suggesting that ZTF-22 may be involved in controlling *fmo-2* levels through *hif-1, nhr-49,* and *mdt-15.* These findings suggest that ZTF-22 is not only specific for *gst-4* and *sod-3* but also plays an important role in the regulation of other detoxification genes.

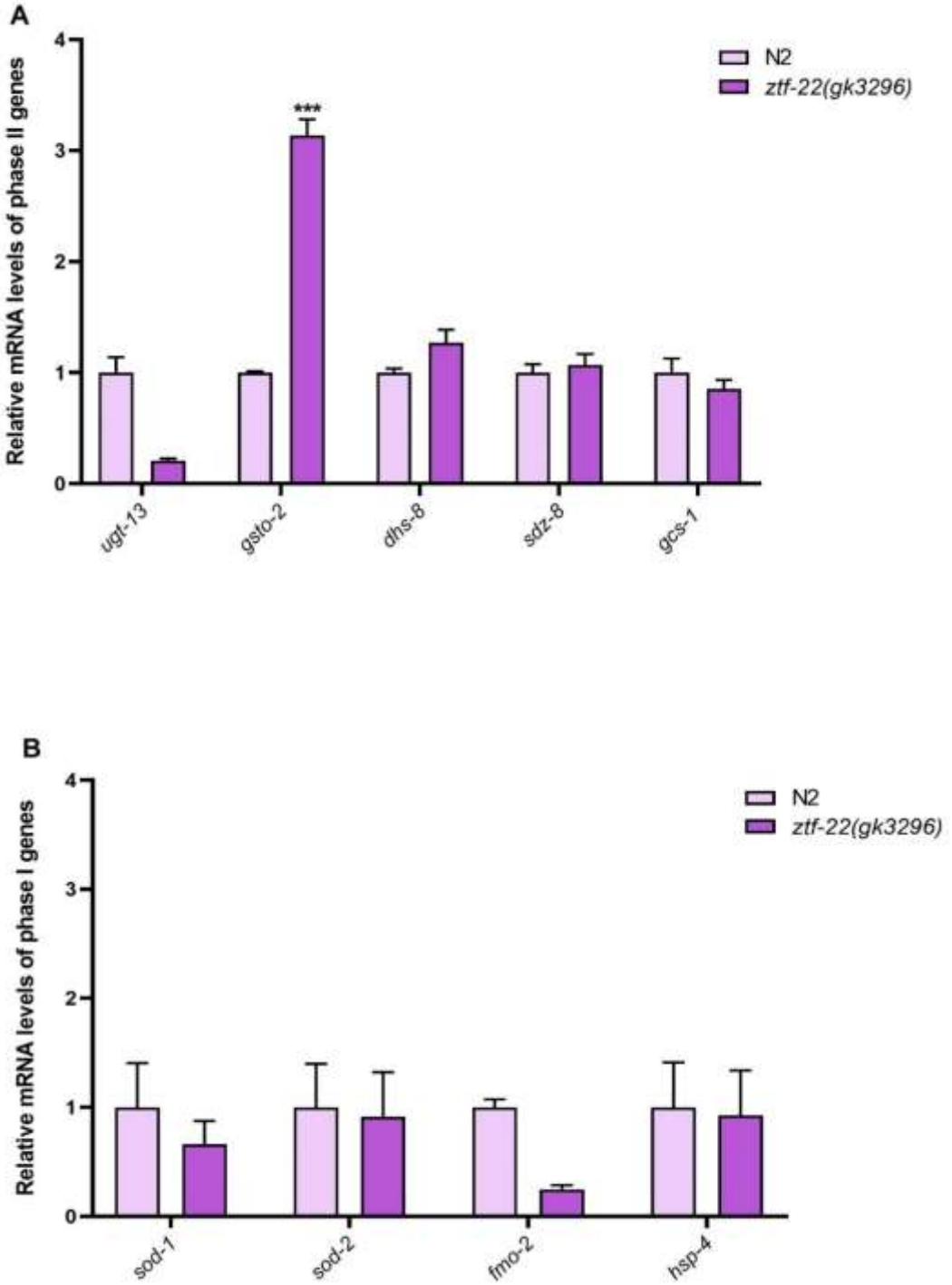

Figure 3.3: *ztf-22* mutation influences the expression of various detoxification genes

qRT-PCR was performed to determine the effect of *ztf-22* mutation on phase II and non-phase II detoxification genes. (A) The relative mRNA levels of phase II detoxification genes. (B) The relative mRNA levels of non-phase II detoxification genes. Relative mRNA levels were normalized to the *tba-1* reference gene. Statistical analysis was carried out using Multiple t-tests. Error bars represent ± SEM; *** $P < 0.001$.

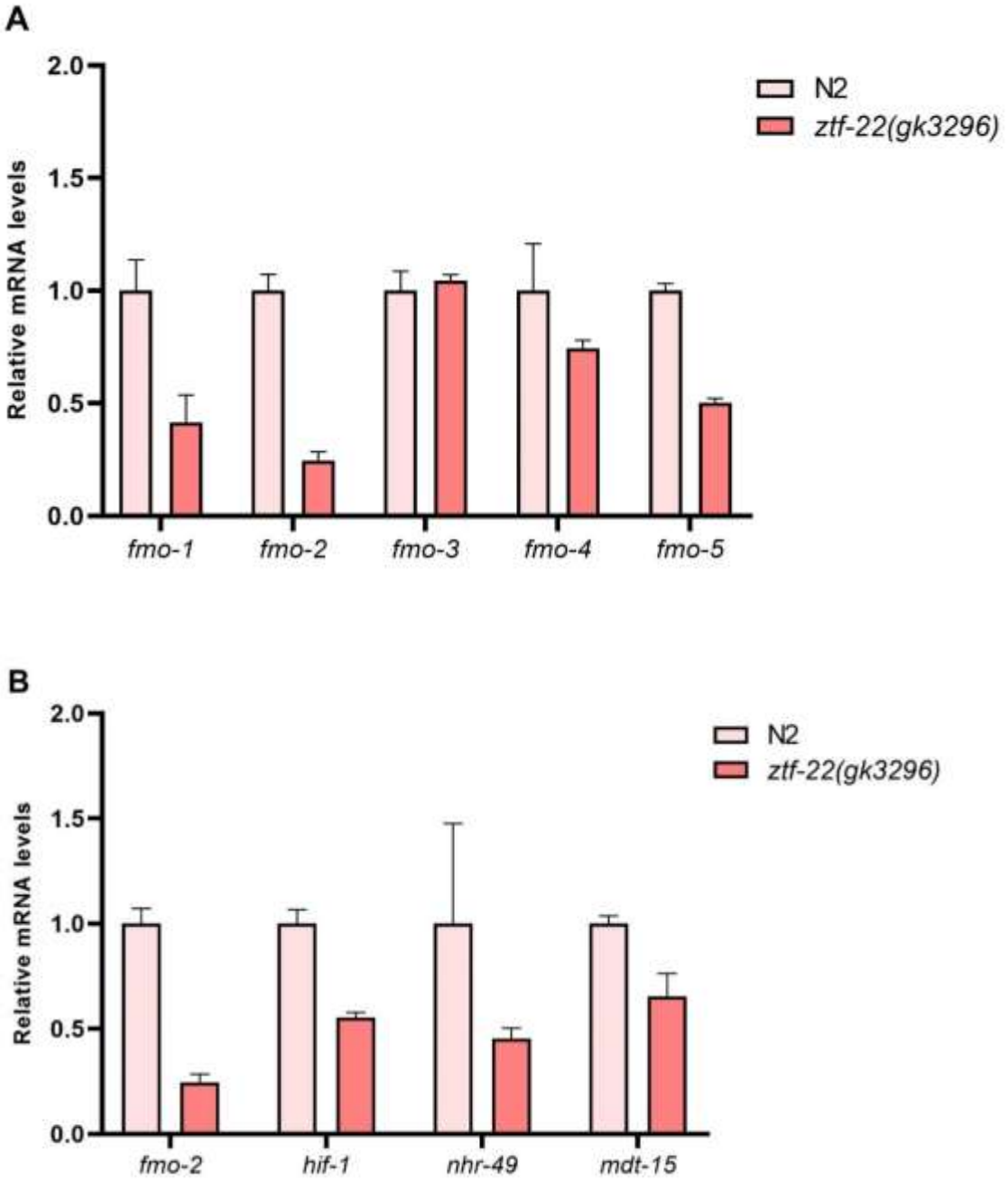

Figure 3.4: *ztf-22* affects the expression of *fmo* genes, and the genes involved in the transcription of *fmo-2.*

(A) shows the mRNA levels of *fmo* family genes. (B) represents the relative mRNA levels of the genes involved in the transcription of *fmo-2*. Relative mRNA levels were normalized to the *tba-1* reference gene. Statistical analysis was carried out using Multiple t-tests. Error bars represent ± SEM.

3.3 *ztf-22* mutants show no significant change in response to oxidative stress induced by sodium arsenite and *tert*-butyl hydroperoxide (*t*BHP) as compared to N2 worms

The *ztf-22(gk3296)* mutants expressed enhanced levels of detoxification genes compared to wild-type worms. To determine whether this would confer an advantage to these worms against oxidative stress, I performed the oxidative stress assay using two different types of stress-inducing agents: sodium arsenite (As) and *tert*-butyl hydroperoxide (*t*BHP).

For the As assay, *ztf-22(gk3296)* mutants and N2 worms were exposed to 5mM As solution. The experiment was set up in the 24-well plate where 3 wells contained 5mM As solution containing either *ztf-22(gk3296)* mutants or N2 worms and one well had M9 buffer containing either *ztf-22(gk3296)* mutants or N2 worms serving as the control. Worms were scored every hour and the ones that did not respond to prodding were considered dead. *ztf-22(gk3296)* mutants showed resistance in the beginning but slowly caught up with N2 worms and reached 100% mortality at the 15th hour mark. The worms in the M9 buffer stayed alive throughout the experiment. The result of this assay shows a trend where *ztf-22(gk3296)* worms appear to be showing some resistance against the oxidative stress induced by As in the beginning of the assay, however, the difference between their survival under the As stress is not statiscally significant. The Kaplan-Meier plot (Figure 3.5A) shows the survivability of the two strains where N2 is represented by a red solid line whereas *ztf-22(gk3296)* mutants are represented by a green solid line. The dotted red and green lines represent the control groups (worms in the M9 buffer). The experiment was performed three times in triplicates and analyzed using the Log-rank (Mantel-Cox) test.

To determine the effect of *t*BHP on *ztf-22(gk3296)* mutants and N2 worms, agar plates with infused *t*BHP solution were poured. Worms were placed on unseeded *t*BHP and NGM plates and

scored every hour. The worms on the control plate survived throughout the experiment. L4 N2 and *ztf-22(gk3296)* worms were placed on 7.5 mM *t*BHP plates and counted every hour. For the first two hours, worms would try to run away from the plate and end up on the wall where they would dry out and die. Therefore, they had to be constantly monitored and brought back to the center for the first 2 hours. As the time progressed, worms became slower and less active. The worms that were unresponsive to poking by wormpick were considered dead. The Kaplan-Meier plot (Figure 3.5B) shows results of this experiment. N2 worms are represented by solid red curve whereas *ztf-22(gk3296)* worms are represented by the solid blue curve. The control group for each strain is represented by red (N2 strain) and blue (*ztf-22* mutants) dotted lines. No statistically significant difference was observed in their survival against *t*BHP as both strains reached 100% mortality around the same time. The experiment was performed three times in triplicates and analyzed using the Log-rank (Mantel-Cox) test.

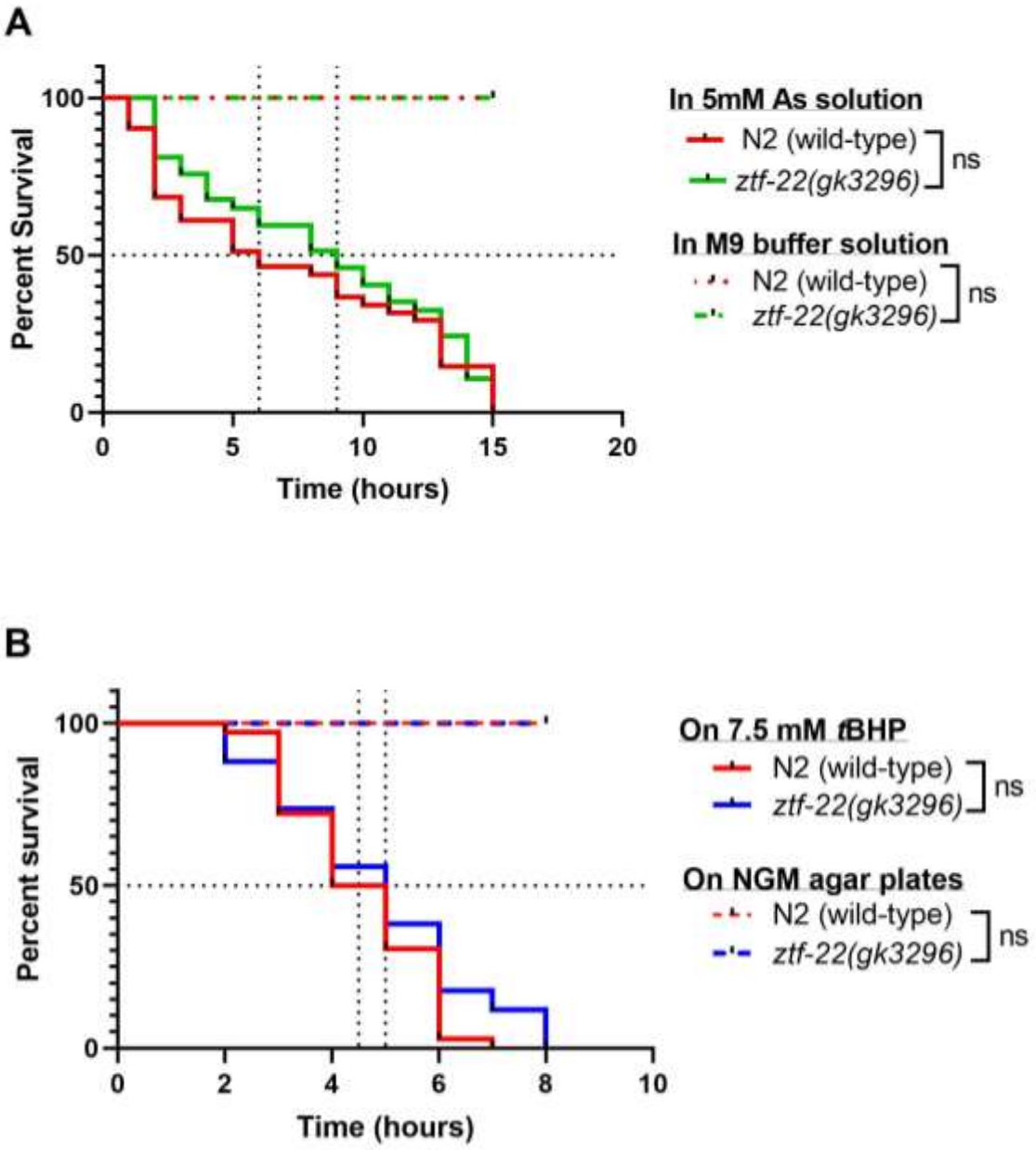

Figure 3.5: *ztf-22(gk3296)* mutants showed short-term resistance against sodium arsenite and *t*BHP compared to N2 worms

(A) Survival plot of the As-assay comparing *ztf-22(gk3296)* mutants to wild-type (N2) worms in 5mM As solution. M9 buffer was used as control. The experiment was set up to have triplicates. A total of 36 worms from each strain were used for this experiment. For statistical details, please refer to table 2. (B) Survival plot of the *t*BHP-assay. The *t*BHP plates were prepared with 7.5mM of *t*BHP whereas the NGM agar plates were used as control. The experiment was set up to have triplicates. A total of 36 worms from each strain were used for this experiment. For statistical details, please refer to Table 3. Kaplan-Meier test and Log-rank (Mantel-Cox) test were used to calculate the survival function and statistical significance respectively for both assays. Data represents one trial.

3.4 *ztf-22* mutation significantly prolongs the lifespan of *C. elegans*

To determine whether *ztf-22(gk3296)* mutation influenced the lifespan of worms, I conducted longevity assays. I followed both strains since they were eggs to see which one lives longer. *ztf-22(gk3296)* mutants show slower development than N2 worms as they mature later and also appear slightly smaller in size. Worms were regularly transferred to fresh plates to avoid crowding, starvation, and desiccation. I used 50 worms per strain for this assay; however, the worms that had died due to reasons other than old age (explosion, desiccation, etc.) were excluded from the total sample size. The Kaplan-Meier plot (Figure 3.6) shows the survivability of the two strains over time where N2 is represented by a solid purple line whereas *ztf-22(gk3296)* mutants are represented by a solid green line. On average, N2 worms have a median lifespan of 19 days whereas *ztf-22(gk3296)* worms have a median lifespan of 21 days. This experiment revealed that the *ztf-22(gk3296)* mutants live significantly longer than the wild-type worms suggesting that ZTF-22 plays an essential role in aging. The data was obtained from three independent trials and analyzed using the Log-rank (Mantel-Cox) test.

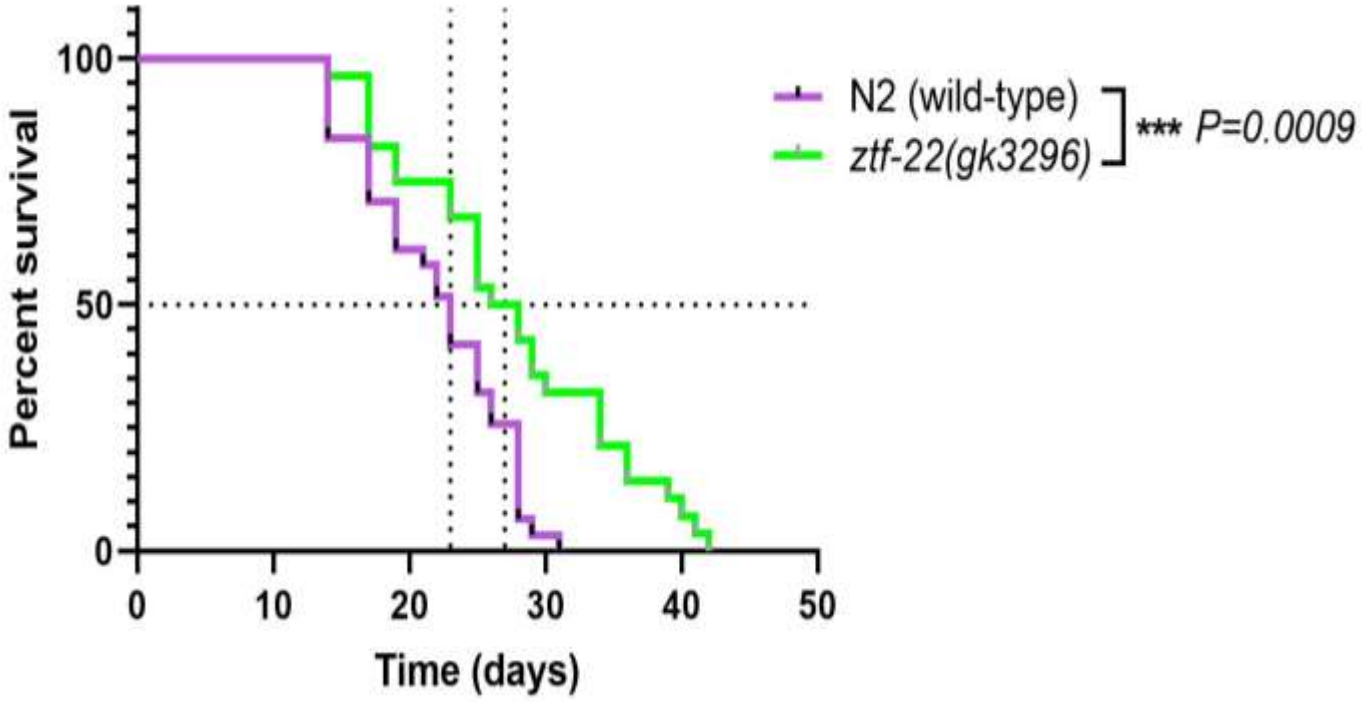

Figure 3.6: *ztf-22(gk3296)* mutants live significantly longer than N2 worms.

Survival curve presenting the lifespan of wild type (purple curve) and *ztf-22(gk3296)* mutant worms (green curve). A total of 50 worms (n=50) were used from each strain to conduct this experiment, however, the worms that died due to reasons other than aging were excluded from the sample size leaving behind 42 N2 and 39 *ztf-22(gk3296)* mutant worms. The estimates of the survival functions are calculated using the Kaplan-Meier method whereas the Log-rank (Mantel-Cox) test was used to calculate significance and P-values; *** $P < 0.001$. Data represents one trial. Please refer to table 4 for statistical details.

3.5 *ztf-22* mutants are more sensitive to heat stress than the N2 worms

In order to determine whether ZTF-22 has any effect on the survival of worms under heat stress, a thermotolerance assay was carried out. Both strains were placed on NGM plates which were put in the 37 ^{O}C incubator. The worms on the plates were scored every hour. The worms were active at the beginning of the experiment but gradually slowed down as time progressed. *ztf-22(gk3296)* mutants showed reduced mobility sooner than the N2 worms. *ztf-22(gk3296)* mutants showed sensitivity to heat stress as all the worms were dead by the 9th hour mark while more than 50% of N2 worms were still alive (Figure 3.7). The controls worms lived throughout the experiment. The experiment was set up to have triplicates and performed three times in total. The graph below represents single trial. *ztf-22(gk3296)* mutants are represented by turquois curve whereas N2 worms are represented by the pink curve. Statistical analysis was performed using the Log-rank test and the Kaplan Meier method.

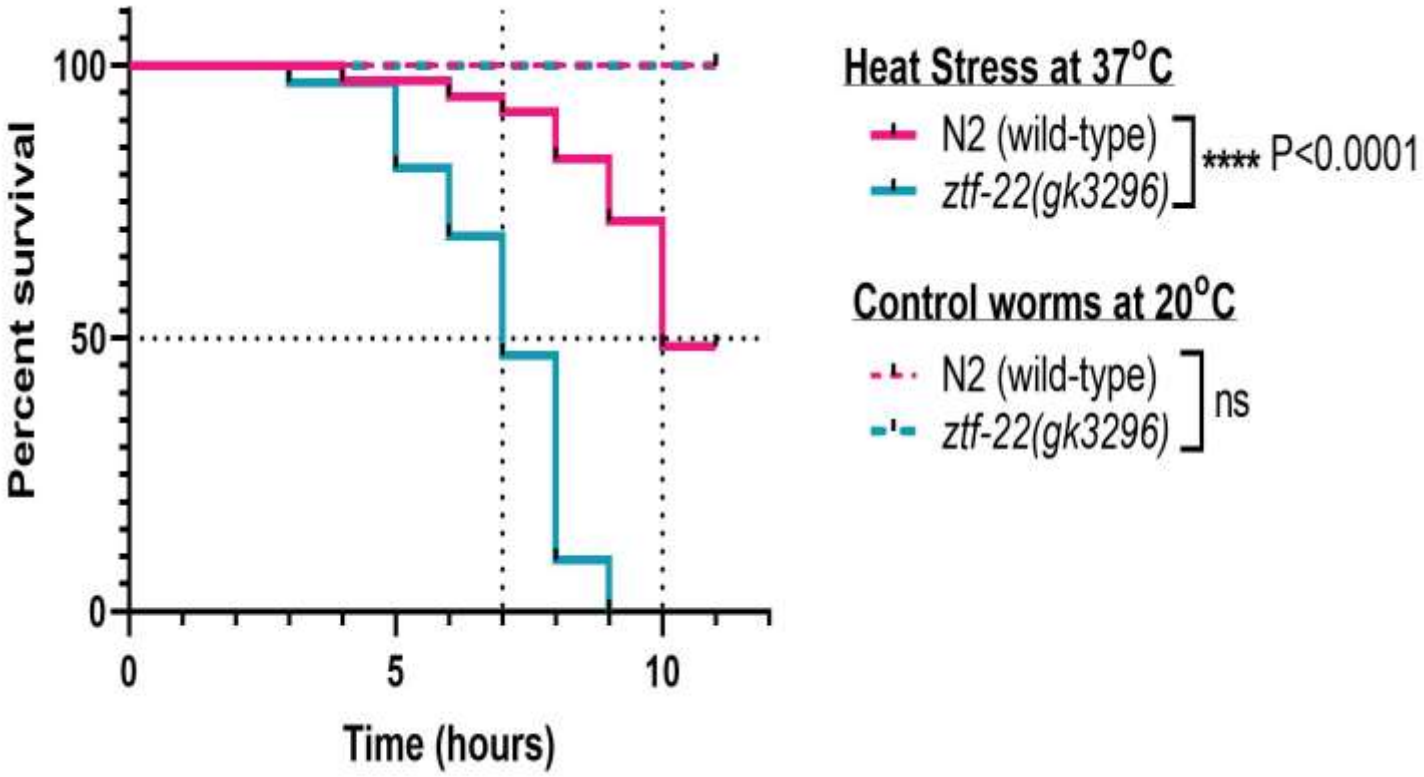

Figure 3.7: The *ztf-22(gk3296)* mutants are less resistance to heat stress than the N2 worms.

The wild-type (N2) worms are shown by the pink curve whereas the *ztf-22(gk3296)* mutants are represented by the turquois color. Worms from both strain (36 worms from each strain) were placed in NGM plates which were placed in the 37 ^{O}C incubator whereas worms placed in NGM plates at 20 ^{O}C served as the control group. The *ztf-22(gk3296)* strain showed significant sensitivity towards heat as all the worms reached 100% mortality by hour 9 whereas more than half of N2 worms were still alive. The experiment was set up to have triplicates. For statistical details, please refer to Table 5. Kaplan-Meier test and Log-rank (Mantel-Cox) test were used to calculate the survival function and statistical significance and P-values; **** $P < 0.0001$. Data represents one trial.

3.6 *ztf-22* mutants show more resistance to Endoplasmic reticulum (ER) stress induced by DTT than the wild type worms

To learn whether ZTF-22 played a role in ER stress, an ER stress assay was performed using dithiothreitol (DTT). 10 mM DTT plates were prepared one day before the experiment. L4 N2 and *ztf-22(gk3296)* worms were placed on DTT plates and worms were counted every hour. For the first hour and a half, worms were constantly monitored as they would stray away from the center and desiccate on the wall of the plate. After a couple of hours, they slowed down and were scored hourly. Worms under DTT stress would appear stubby, shrunk, and exploded at the touch of the wormpick releasing all of their body content on to the plate. When worms reached this stage, they were considered dead. NGM plates without DTT served as control plates. *ztf-22(gk3296)* mutants lived significantly longer than the wild-type worms (Figure 3.8). N2 worms reached 100% mortality by hour 11 whereas more than 50% of *ztf-22(gk3296)* were still alive by this time. The controls worms lived throughout the experiment. The experiment was set up to have triplicates and performed three times in total. The graph below represents one trial. *ztf-22(gk3296)* mutants are represented by yellow curve whereas N2 worms are represented by red curve. Long-rank test and Kaplan-Meier test were used to perform statistical analysis.

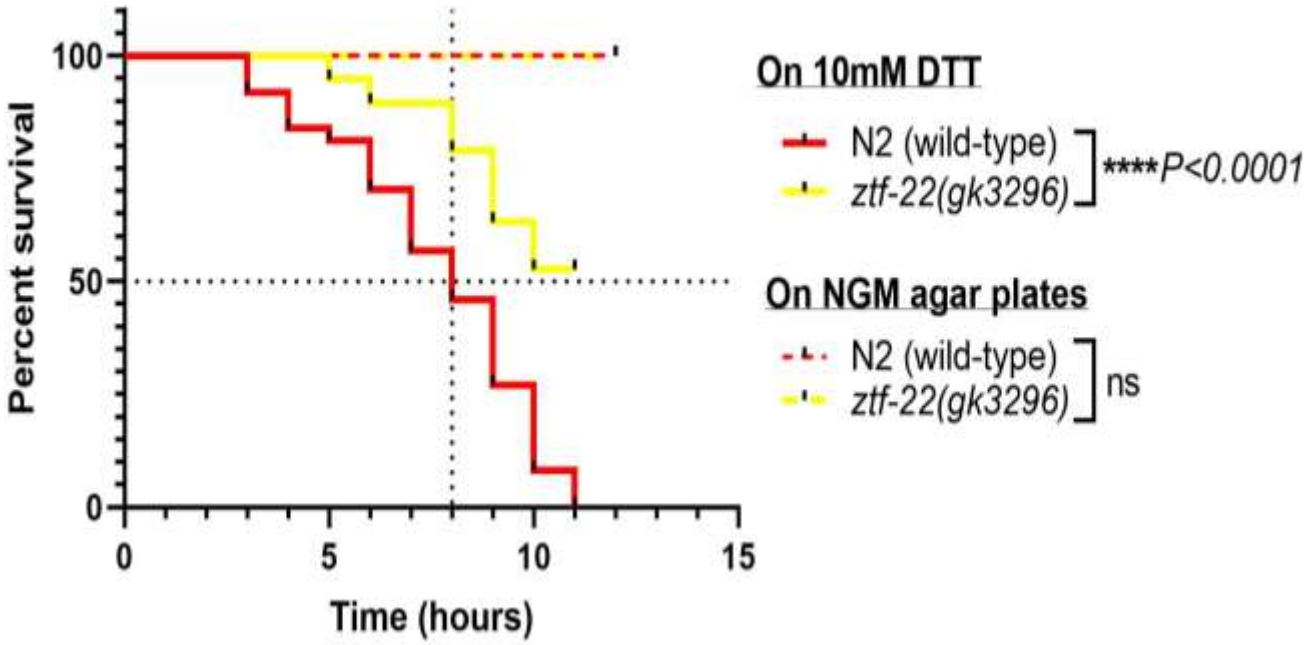

Figure 3. 8: *ztf-22(gk3296)* mutants show resistance towards ER stress induced by 10 mM DTT.

N2 (wildtype) worms are represented by red curve whereas the *ztf-22(gk3296)* mutants are represented by yellow curve. A total of 36 worms from each strain were used in this experiment. The worms were placed on 10 mM DTT plates and counted every hour. Regular NGM plates that did not contain DTT served as control plates. As seen from the graph, *ztf-22(gk3296)* worms showed significant resistance to ER stress. The experiment was set up to have triplicates. For statistical details, please refer to Table 6 . Kaplan-Meier test and Log-rank (Mantel-Cox) test were used to calculate the survival function, statistical significance, and P-values; **** $P < 0.0001$. Data represents one trial.

CHAPTER 4: DISCUSSION

4.0 Discussion:

4.1 Summary

The main purpose of this project was to determine the role of ZTF-22 in oxidative stress response and its biological role in the cell in terms of resistance against oxidative stress and lifespan in *C. elegans* . By the end of this project, I have learned that (1) ZTF-22 acts as a negative regulator of the PII detoxification gene, *gst-4.* (2) It also regulates the expression of other PII (*gsto-2*, and *ugt-13*) and non-phase II genes (*sod-3, fmo-1, fmo-2, fmo-4* and *fmo-5*). (3) *ztf-22* mutation confers short-term resistance against oxidative stress induced by sodium arsenite but does not provide resistance against *t*BHP. (4) *ztf-22* plays an important role in longevity as its deletion causes a considerable extension of lifespan in *C. elegans* . (5) *ztf-22(gk3296)* mutants are more sensitive to heat stress than the N2 (wildtype) worms. (6) *ztf-22* mutation provides resistance against the ER stress induced by DTT.

4.1 ZTF-22 negatively regulates PII and PI genes potentially through SKN-1 and DAF-16

Previously, our lab demonstrated that *brap-2(ok1492)* mutants exhibited increased localization of SKN-1/Nrf2 in intestinal nuclei and elevated expression of SKN-1-dependent PII detoxification genes (81). Among these PII genes, the basal expression level of *gst-4* was enhanced quite significantly by the *brap-2(ok1492)* mutation. Furthermore, our lab performed a transcription factor-specific RNAi screen revealing ZTF-22 to be a repressor of *gst-4* because RNAi knockdown of ZTF-22 enhanced *gst-4* expression. As a result of this RNAi screen, the uncharacterized transcription factor, ZTF-22, was selected for the investigation of its role in the context of oxidative stress and to identify its general biological role in the cell regarding longevity and survival under various stress-induced conditions.

After learning that loss of ZTF-22 induced expression of *gst-4*, I used molecular and genetic techniques to determine whether ZTF-22 was only specific for *gst-4* expression, or it has a general effect on PII as well as non-phase II detoxification genes. I was able to determine that expression of PII detoxification genes such as *gst-4* and *gsto-2* were elevated whereas *ugt-13* expression was reduced in *ztf-22(gk3296)* mutants. This finding suggested that ZTF-22 has a general effect on detoxification genes and is not specific to only *gst-4*. GSTs play a crucial defensive role against oxidative stress induced by ROS and *gst-4* is a direct target of SKN-1 (106). Thus, ZTF-22 was proposed to be a potential regulator of SKN-1 and responsible for controlling SKN-1 through SKN-1 signaling pathways.

The enhanced expression of PII genes in *ztf-22* mutants suggests that these worms may be more resistant to oxidative stress induced by different reagents such as sodium arsenite (As) and *tert*-butyl hydroperoxide (*t*BHP). As induces oxidative stress by the overproduction of ROS through the mitochondria (107) whereas *t*BHP causes oxidative stress by attacking lipids and proteins in the cell (108). Almost all the As-induced detoxification enzymes are SKN-1 dependent, however, those induced by *t*BHP tend to be both SKN-1 dependent and SKN-1 independent (108). The *ztf-22(gk3296)* mutants show initial resistance against As, however, both strains reach 100% mortality around the same time. On the other hand, resistance against *t*BHP appears to be only temporary. The resistance against As seen in *ztf-22* mutants could be attributed to having high *gst-4* and *gsto-2* levels which are SKN-1 dependent PII detoxification genes. Since *t*BHP-induced stress partially depends on SKN-1, that is most likely why *ztf-22* mutants show only temporary resistance against *t*BHP. Although I predicted *ztf-22* mutants to exhibit enhanced survival against both stressors due to the presence of elevated PII genes but possibly due to reduced levels of *ugt-13*, *ztf-22(gk3296)* mutants did not show increased survival against As and *t*BHP as it was

anticipated. *ugt-13* is also a major PII detoxification enzyme that protects against ROS-induced stress and the absence of resistance against oxidative stress-inducing agents, As and *t*BHP, could be ascribed to low levels of *ugt-13* in *ztf-22(gk3296)* mutants. The observation that some of the SKN-1 target genes were enhanced (*gst-4, gsto-2*), while some were reduced (*ugt-13*), and some remained unchanged (*dhs-8, gcs-1, sdz-8*) demands for further investigation. Another observation made in *ztf-22(gk3296)* mutants was the downregulation of *fmo* genes. The Flavin-containing monooxygenases (FMOs) are xenobiotic metabolizing enzymes that increase the solubility and excretion of xenobiotics by adding an oxygen molecule to nitrogen, sulfur, or other nucleophilic atoms (99,109,110). Huang *et al*. (111) demonstrate that increased FMO expression renders worms resistant to stress against As. The probable explanation for why *ztf-22(gk3296)* did not show strong resistance against As and *t*BHP could be that high expression of *gst-4* and *gsto-2* and low expression of *ugt-13* and *fmo* genes balanced each other out and rendered *ztf-22(gk3296)* only slightly resistant towards stress against As.

I also examined the levels of PI genes and found that *sod-3*, which lies under the control of DAF-16, portrayed increased expression in *ztf-22(gk3296)* worms. Higher expression of *sod-3* in *ztf-22(gk3296)* mutants suggested a possibility that ZTF-22 may potentially be regulating *sod-3* via DAF-16. Moreover, the prolonged lifespan observed in various strains of *C. elegans* appears to be dependent on DAF-16 (112). Since *ztf-22(gk3296)* mutants show an extended lifespan, as well as enhanced levels of *sod-3*, this gives a good indication that ZTF-22 could be a negative regulator of DAF-16.

It is possible that ZTF-22 may potentially be an important component of the IIS pathway or the MAPK pathway since both of these pathways regulate SKN-1 and DAF-16. Therefore, the possibility exists that ZTF-22 may be controlling both transcription factors by either stimulating

the IIS pathway or inhibiting the MAPK pathway. Regardless, one conclusion from this project is that ZTF-22 regulates the transcription of PI and PII genes potentially through SKN-1 and DAF-16 (Figure 4.1). The piece of the puzzle that needs further research would be to determine where ZTF-22 specifically fits in these signaling cascades to control the function of SKN-1 and DAF-16 and consequently their target genes and their phenotypes.

4.2: The biological role of ZTF-22 in *C. elegans* beyond oxidative stress

Similar to oxidative stress, heat stress is also managed by the IIS pathway. The Heat Shock Transcription Factor (HSF-1) controls various heat response genes and is negatively regulated by the IIS pathway. Since I presumed ZTF-22 may be stimulating IIS pathway to negatively regulate SKN-1 and DAF-16, I was curious to learn whether *ztf-22* mutation imparted resistance against heat stress. Based on this observation, I predicted *ztf-22(gk3296)* mutants to show resistance against heat stress when exposed to a temperature of 37 ^{O}C. My prediction, however, was contrary to the actual results as my *ztf-22(gk3296)* mutants showed increased sensitivity to heat stress. This suggests that ZTF-22 is crucial for survival at high temperatures. HSF-1 is negatively regulated by DDL-1/2 in the IIS pathway and it has been shown that inhibition of DDL-1/2 not only increases thermotolerance but also induces longevity in worms (46). My *ztf-22(gk3296)* mutants show conflicting results in this regard as they show increased longevity but reduced thermotolerance suggesting that ZTF-22 potentially acts as an activator of HSF-1 and the loss of ZTF-22 rendered *ztf-22(gk3296)* mutants highly sensitive to high temperatures. However, the longevity phenotype of *ztf-22(gk3296)* mutants is probably dependent on DAF-16 and SKN-1 but independent of HSF-1. This finding suggests that if ZTF-22 is indeed working through IIS pathway, it is exerting its negative influence towards SKN-1 and DAF-16 downstream of DAF-2. This is because if ZTF-22 were directly stimulating DAF-2, then the absence of ZTF-22 would have increased the expression

of heat response gene by the activation of HSF-1 thus rendering *ztf-22(gk3296)* mutants resistance against heat stress rather than sensitive relative to N2 worms as seen in this case.

If ZTF-22 regulates detoxification genes through SKN-1 then the effect of *ztf-22* mutation should also be observed outside of oxidative stress with regards to its influence on SKN-1. SKN-1 is prominently known for its role in protecting against oxidative stress and inducing longevity, however, it also plays a major role in alleviating ER stress which is caused by the build-up of misfolded proteins in the rough ER (113). When the ER undergoes stress, this triggers the Unfolded Protein Response (UPR). This response diminishes ER stress by decreasing protein translation, expanding ER size and folding capacity, and triggering the degradation of unfolded proteins in the cytosol (77). I was interested in determining whether my *ztf-22(gk3296)* mutants would show resistance against ER stress. To investigate this, I carried out an ER stress assay using DTT which induces ER stress by preventing disulfide bond formation in the ER (77). DTT treatment has been shown to induce SKN-1 activation and many of its target genes and also increases SKN-1 protein levels (77). Under ER stress, SKN-1 is essential in inducing the activation of core UPR signaling and transcription factors (77). I found my *ztf-22(gk3296)* worms highly resistant to ER stress which could potentially be attributed to the high expression of SKN-1 in *ztf-22(gk3296)* mutants.

These survival experiments reveal a broader role for ZTF-22 beyond oxidative stress, including roles in longevity, thermotolerance, and ER stress. My current speculation is that ZTF-22 may be regulating the aforementioned processes through signaling cascades controlling SKN-1 and DAF-16. These two master transcription factors participate in a wide variety of processes in the cell. Based on this assumption, I believe that the role of ZTF-22 is not limited to oxidative stress response, but it is involved in a broad range of activities in the cell.

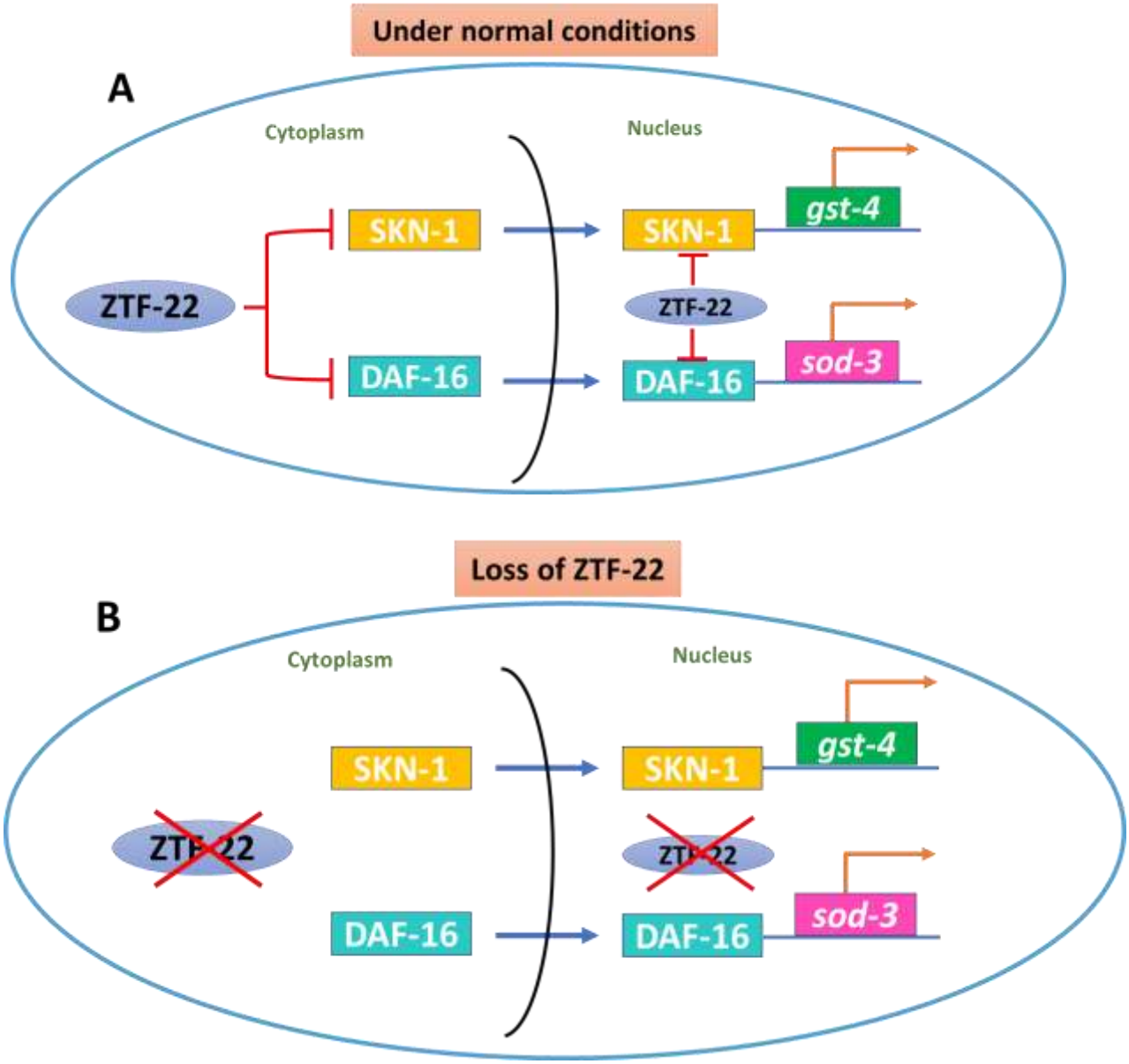

Figure 4.1: The proposed model for the function of ZTF-22 in the regulation of PI and PII detoxification genes.

(A) Under normal conditions, ZTF-22 negatively regulates PII and PI genes (*gst-4* and *sod-3*) potentially through SKN-1 and DAF-16 transcription factors either by direct or indirect inhibition. ZTF-22 could be present in the cytoplasm or the nucleus to negatively regulate the two transcription factors. However, under the conditions when ZTF-22 is lost, SKN-1 and DAF-16 induce the transcription of their target PII and PI detoxification genes.

4.3 Future work to further investigate the function of ZTF-22:

This project has successfully revealed an important role of ZTF-22 in the context of oxidative stress involving *gst-4*. Through RNAi, transgenesis and qPCR, I showed that ZTF-22 acts as a repressor for *gst-4*. However, the precise mechanism through which it regulates *gst-4* remains to be elucidated. It is possible that ZTF-22 controls *gst-4* through SKN-1 either by physically interacting with SKN-1 or through its indirect inhibition. It is also possible that ZTF-22 may be regulating *gst-4* expression by interacting with one of the upstream regulators of SKN-1 through one of the signaling pathways that control activation of SKN-1 such as the canonical IIS pathway or the MAPK pathway. Another possibility that could explain working of ZTF-22 is that ZTF-22 might be required for the expression of microRNAs that regulate *skn-1* mRNA.

To address the possibility that ZTF-22 directly regulates SKN-1 activation, we could generate double mutants of *ztf-22* mutant worms along with a deletion in some of the upstream regulators of SKN-1 (*pmk-1, mpk-1, mek-1, and sek-1*) and then measure *gst-4* mRNA levels using qPCR. The aim is to determine whether these pathways are required for the enhanced expression of *gst-4* that is seen in *ztf-22* mutants. We could also use phospho-specific antibodies for p38 (*pmk-1* in *C. elegans*) and MAPK (*mpk-1*) to determine if these pathways are activated in *ztf-22* mutants, causing an increase in SKN-1 activity and *gst-4* expression.

To address the possibility that ZTF-22 works directly on PII detoxification gene promoters to repress their expression, we could carry out the Luciferase assay. We can use the *gst-4* promoter luciferase reporter construct (already made by our lab) for expression in mammalian cell culture. This construct will be co-transfected with constructs expressing ZTF-22 and SKN-1into HEK-293T cells. Our lab has previously shown that SKN-1 can promote luciferase production from the

gst-4 promoter, so I will determine if ZTF-22 can directly repress this activity in mammalian cell culture.

To investigate the possibility that ZTF-22 may be responsible for expressing a microRNA that regulates *skn-1* mRNA, RNA-sequencing could be done to determine which genes are upregulated or downregulated in N2 and *ztf-22* deletion mutants. The aim is to identify potential candidates that may be involved in the increased oxidative stress response when *ztf-22* is knocked down. To explore the possibility that *ztf-22* may also express a miRNA that is implicated in SKN-1 translation, we intend to look at the transcriptome of *ztf-22* mutant worms for decreased expression of miRNA that could potentially regulate *skn-1* mRNA.

5.0 Conclusion:

BRAP-2 is hypothesized to be a cytoplasmic retention protein for SKN-1 and prevents the activation of SKN-1 dependent PII genes such as *gst-4*. Knockdown of *brap-2* shows elevated expression of *gst-4*. This project has revealed another transcription factor, ZTF-22, the knockdown of which also results in enhanced expression of *gst-4*. ZTF-22 also showed regulation of other PII and non-phase II genes, besides *gst-4*, indicating that ZTF-22 plays an important role in oxidative stress response by regulating various detoxification genes. In addition to its role in oxidative stress response, ZTF-22 also appears to be a major player in longevity as its deletion prolongs lifespan of *C. elegans* quite significantly. Moreover, ZTF-22 is required to survive under heat stress and plays a major role in ER stress where loss of ZTF-22 rendered *ztf-22(gk3296)* worms resistant to induced ER stress.

Based on these finding, ZTF-22 appears to be an essential protein required for various cellular activities in *C. elegans* . The human ortholog of ZTF-22 is currently unknown, however,

the genes that it influences (*gst-4*, *ugt-13*, and the *fmo* genes) have counterparts in other organisms including humans (HPGDS, UGT1A10, FMOs). More work is required to better understand ZTF-22 with regards to its link to major transcription factors, SKN-1 and DAF-16. Once this link has been established, ZTF-22 could potentially be used as a target of therapeutic interventions needed to cure various oxidative stress linked diseases.

APPENDIX

Table 1. List of mammalian homologs of *C. elegans* genes and their functions.

The *C. elegans* genes investigated in this project are listed here. The primary source of this information was Wormbase **(114)**.

C. elegans gene	Mammalian homolog	Description of function in *C. elegans*
age-1 (AGEing alteration)	Phosphatidylinositol-4,5-bisphosphate 3-kinase catalytic subunit α and δ **(PIK3CA and PIK3CD)**	– Involved in dauer entry; determination of adult lifespan; and regulation of synaptic assembly at neuromuscular junction
akt-1/2 (AKT kinase family)	AKT serine/threonine kinase 1 and 2 **(AKT1 and AKT2)**	– Enables calmodulin binding activity; phosphatidylinositol-3,4,5-trisphosphate binding activity; and protein serine/threonine kinase activity – Involved in determination of adult lifespan; protein phosphorylation; and signal transduction
brap-2 (BRCA1 associated protein)	BRCA1 associated protein 2 **(BRAP2)**	– Loss of *brap-2* mutants are sensitive to oxidizing conditions – Involved in DNA damage induced germline apoptosis, and insulin signaling pathway.
cdc-42 (Cell Division Cycle related)	Cell Division Cycle 42 **(CDC42)**	– Involved in establishment of mitotic spindle orientation; positive regulation of nematode male tail tip morphogenesis; and regulation of cellular component organization
daf-16 (abnormal DAuer formation 16)	Forkhead box O **(FOXO1, FOXO3, and FOXO4)**	– Enables 14-3-3 protein binding activity; beta-catenin binding activity; and enzyme binding activity – Involved dauer formation, longevity, stress response, and metabolism
daf-2 (abnormal DAuer Formation)	Insulin like growth factor 1 receptor **(IGF1R)**	– Enables PTB domain binding activity, SH2 domain binding activity, and protein kinase binding activity – Involved in dauer exit, regulation of developmental process, and regulation of macromolecule metabolic process.

		– Has a negative effect on protein import into nucleus.
dhs-8 (DeHydrogenases, Short chain)	WW domain containing oxidoreductase **(WWOX)**	– Phase II detoxification enzymes that defends against ROS.
fmo-1/2/3/4/5 ((Flavin-containing MonoOxygenase family)	Flavin containing dimethylaniline monooxygenase 2/3/4 **(FMO2/3/4)**	– Involved in lipid metabolic process – Involved in xenobiotic metabolism
gcs-1 (gamma GlutamylCysteine Synthetase)	Glutamate-cysteine ligase catalytic subunit **(GCLC)**	– Enables glutamate-cysteine ligase activity – Involved in glutathione biosynthetic process, response to arsenic-containing substance; and response to superoxide.
gst-4 (Glutathione-*S*-transferase)	Hematopoietic prostaglandin D synthase **(HPGDS)**	– Enables glutathione transferase activity – Involved in the detoxification of ROS
gsto-2 (Glutathione S-Transferase, Omega class)	Glutathione-S-transferase omega 1/2 **(GSTO1/2)**	– Enables glutathione dehydrogenase (ascorbate) activity and glutathione transferase activity – Involved in the detoxification of xenobiotics
hif-1 (Hypoxia Inducible Factor)	Endothelial PAS demain protein 1 **(EPAS1)** hypoxia inducible factor 3 subunit alpha **(HIF3A)**	– Enables DNA-binding transcription factor activity and RNA polymerase II-specific DNA-binding transcription factor binding activity – Involved in cellular response to caloric restriction, determination of adult lifespan, and heat acclimation
him-5 (High Incidence of Males)	N/A	– Involved in X chromosome segregation – *him-5* mutants produce large number of male worms
hsf-1 (Heat Shock Factor)	Heat shock transcription factor 1**(HSF1)**	– involved in the induction of heat response genes in response to elevated temperatures
mdt-15 (MeDiaTor)	Mediator complex subunit 15 **(MED15)**	– Enables nuclear receptor binding activity and transcription coactivator activity – Involved in determination of adult lifespan, nematode larval development, and sequestering of triglyceride

nhr-49 (Nuclear Hormone Receptor family)	Hepatocyte nuclear factor 4 alpha **(HNF4A)**	– Involved in determination of adult lifespan and regulation of fatty acid metabolic process
sdz-8 (SKN-1 Dependent Zygotic transcript)	Carbonyl reductase 3 **(CBR3)**	–
skn-1 (SKiNhead)	Nuclear factor erythroid 2-related factor 2 **(Nrf2)**	– Involved in endodermal development, oxidative stress response, longevity, and ER stress response
sod-1 (Superoxide dismutase)	Superoxide dismutase 1 **(SOD1)**	– Enables copper ion binding activity, protein homodimerization activity, and superoxide dismutase activity – Involved in regulation of brood size, regulation of vulval development, and response to oxidative stress
sod-2		
sod-3 (Superoxide dismutase)	Superoxide dismutase 2 **(SOD2)**	– Enables protein homodimerization activity and superoxide dismutase activity – Involved in removal of superoxide radicals.
tra-1 (TRAnsformer: XX animals into males)	GLI family zinc finger **(GLI1, GLI2, GL3)**	– Enables RNA polymerase II cis-regulatory region sequence-specific DNA binding activity, RNA polymerase II intronic transcription regulatory region sequence-specific DNA binding activity, and protein C-terminus binding activity – Involved in developmental and reproduction, negative regulation of transcription by RNA polymerase II, and positive regulation of neuron apoptotic process
ugt-13 (UDP-GlucuronosylTransferase)	UDP glucuronosyltransferase family 1 member A10 **(UGT1A10)**	– PII detoxification enzymes involved in protection against oxidative stress
wdr-23 (WD Repeat protein)	DDB1 and CUL4 associated factor 11 **(DCAF11)**	– Negative regulator of SKN-1 – Involved in determination of adult lifespan, negative regulation of cellular response to manganese ion, and positive regulation of neuron death

ztf-17 and *ztf-22* (Zinc finger putative Transcription Factor family)	ZFP42 zinc finger Protein **(ZFP42/REX1)**	– Involved in oxidative stress response, thermotolerance, longevity and ER stress

Table 2: Statistics for the sodium arsenite assay.

	Strains	No. of samples	Median Survival				Hours at % mortality				
			Hours	SE	95% C.I.	P-value	25%	50%	75%	90%	100%
Trial 1	Wildtype (N2)	36	7.47	0.80	5.91 ~ 9.03		2	8	12	13	15
	ztf-22(gk3296)	36	9.08	0.77	7.58 ~ 10.59	0.0872	4	10	13	15	15
Trial 2	Wildtype (N2)	36	7.36	0.88	5.64 ~ 9.09		2	6	13	15	15
	ztf-22(gk3296)	36	8.31	0.79	6.76 ~ 9.85	0.7641	3	9	13	14	15
Trial 3	Wildtype (N2)	36	8.08	0.98	6.16 ~ 10.01		2	12	14	15	15
	ztf-22(gk3296)	36	8.64	0.89	6.90 ~ 10.38	0.5720	2	9	14	15	15

P values are relative to wild type (N2).

Table 3: Statistics for the *t*BHP survival assay.

	Strains	No. of samples	Median Survival				Hours at % mortality				
			Hours	SE	95% C.I.	P-value	25%	50%	75%	90%	100%
Trial 1	Wildtype (N2)	36	6.58	0.16	6.26 ~ 6.90	-	6	7	8	9	9
	ztf-22(gk3296)	36	6.56	0.18	6.22 ~ 6.91	0.9957	6	7	8	9	9
Trial 2	Wildtype (N2)	36	5.55	0.13	5.29 ~ 5.80	-	5	6	7	8	9
	ztf-22(gk3296)	36	5.59	0.19	5.22 ~ 5.95	0.3889	5	6	7	8	9
Trial 3	Wildtype (N2)	36	4.53	0.21	4.11 ~ 4.95	-	3	4	6	7	8
	ztf-22(gk3296)	36	4.85	0.31	4.24 ~ 5.46	0.1883	3	5	6	8	9

P values are relative to wild type (N2).

Table 4: Statistics for the longevity assay.

	Strains	No. of Samples	Median Survival				Days at % mortality				
			Days	SE	95% C.I.	P-value	25%	50%	75%	90%	100%
Trial 1	Wildtype (N2)	50	17.92	1.13	15.71 ~ 20.13		10	17	25	28	31
	z*tf-22(gk3296)*	50	18.08	1.35	15.43 ~ 20.73	P<0.0001	10	13	25	34	42
Trial 2	Wildtype (N2)	50	19.84	0.74	18.39 ~ 21.29		17	21	24	26	29
	z*tf-22(gk3296)*	50	25.68	1.32	23.08 ~ 28.28	P<0.0001	20	27	33	38	42
Trial 3	Wildtype (N2)	50	18.63	0.79	17.07 ~ 20.19		14	19	23	25	28
	z*tf-22(gk3296)*	50	22.09	0.75	20.62 ~ 23.56	P<0.0001	17	23	26	28	31

P values are relative to wild type (N2).

Table 5. Statistics for the thermotolerance assay.

	Strains	No. of samples	Median Survival				Hours at % mortality				
			Hours	SE	95% C.I.	P-value	25%	50%	75%	90%	100%
Trial 1	Wildtype (N2) exposed to 37^{O}C	36	9.24	0.20	8.84 ~ 9.64	-	8	-	-	-	-
	z*tf-22(gk3296)* exposed to 37^{O}C	36	7.25	0.22	6.82 ~ 7.68	<0.0001	6	7	8	9	10
Trial 2	Wildtype (N2) exposed to 37^{O}C	36	9.36	0.22	8.93 ~ 9.79		9	10	-	-	-
	z*tf-22(gk3296)* exposed to 37^{O}C	36	7.33	0.27	6.80 ~ 7.87	<0.0001	6	8	9	10	9
Trial 3	Wildtype (N2) exposed to 37^{O}C	36	8.33	0.31	7.72 ~ 8.94		7	9	-	-	-
	z*tf-22(gk3296)* exposed to 37^{O}C	36	5.47	0.17	5.14 ~ 5.80	<0.0001	5	6	7	8	9

P values are relative to wild type (N2).

Table 6: Statistics for ER stress assay.

	Strains	No. of samples	Median Survival				Hours at % mortality				
			Hours	Std. error	95 % C.I.	P-value	25 %	50%	75%	90%	100%
Trial 1	Wildtype (N2)	36	5.25	0.31	4.64 ~ 5.86		4	5	7	8	9
	z*tf-22(gk3296)*	36	7.66	0.29	7.08 ~ 8.23	P<0.0001	7	-	-	-	-
Trial 2	Wildtype (N2)	36	7.50	0.38	6.76 ~ 8.24		6	8	9	10	11
	z*tf-22(gk3296)*	36	9.33	0.28	8.79 ~ 9.88	P<0.0001	10	-	-	-	-
Trial 3	Wildtype (N2)	36	6.64	0.33	5.99 ~ 7.29		5	6	7	8	9
	z*tf-22(gk3296)*	36	8.78	0.12	8.53 ~ 9.02	P<0.0001	9	-	-	-	-

P values are relative to wild type (N2).

Table 7: List of *C. elegans* strains used in this project.

Strains	Description
N2	Bristol Wildtype
CF1553	*muls84(sod-3p::gfp)*
CL2166	*dvIs19(gst-4p::gfp)III*
DR466	(*him-5(e1490)V*
YF215	*ztf-22(gk3296)II* backcrosses 1x
YF220	*ztf-22(gk3296)II; dvIs19(gst-4p::gfp)III*
YF224	*ztf-22(gk3296)II; muls84(sod-3p::gfp)*

Table 8: List of primers used for genotyping *ztf-22* with SW-PCR.

Name	Tm (ºC)	Sequence
ztf-22(gk3296)	50.7	TGTGAAAAAGAGCCAAATTGATAA
	51.6	GAGGTTTTTCCTGAAAATTGAAAA

Table 9: List of forward and reverse primers for qRT-PCR.

Genes	Tm (°C)	Sequence
cdc-42	67.6 67.7	F: TCGACAATTACGCCGTCACA R: AGGCACCCATTTTTCTCGGA
dhs-8	64.2 65.4	F: AAAAGGATCGGGTGGGTACA R: AAACGACATGTGCTCCTGCT
fmo-1	57.3 56.8	F: GGAGCCGACTTGGACATGAA R: CACTTGTGCGTGATCGTTCG
fmo-2	64.0 63.5	F: GGAACAAGCGTGTTGCTGT R: GCCATAGAGAAGACCATGTCG
fmo-3	58.1 57.3	F: TTCTTGTTGTGGGTGCTGGG R: TGACCGTTGACAACTCGGTC
fmo-4	56.6 57.3	F: CTCGGCATCGGAAATTCTGC R: TTGGCAACTGCATGAGGGAT
fmo-5	56.7 57.1	F: CAACTTCTTGTGGTCGGTGC R: AACGGTTGACAGGTCCGTTT
gcs-1	63.8 63.8	F: CCAATCGATTCCTTTGGAGA R: GCTACTTCCGGGAATGTGAA
gst-4	64.0 63.6	F: TGCTCAATGTGCCTTACGAG R: AGTTTTTCCAGCGAGTCCAA
gsto-2	66.6 65.5	F: TCCACCAGCTTCAGGAACCA R: TTCCCTCGTCGTGCTCTAGT
hif-1	57.5 55.5	F: TACCTCCCGACCGAAGACAT R: TTGATACTCGGGGGACTGTT
hsp-4	64.1 63.7	F: TGACTCGTGCCAAGTTTGAG R: GCTCCTTGCCGTTGAAGTAG
mdt-15	57.0 57.1	F: GCGAGGCAGGTCGAAGAATA R: CCAGCCGGAGTGTTTCCTAA
nhr-49	57.4 57.4	F: CTGCAACGGGTGTAAGGGAT R: ACTGGCTCCAGATGTTGGTG
sdz-8	64.7 60.4	F: CTGCTGAGGTACGGAACGAA R: TCTGTAFFCGACAACTGGGA
sod-1	65.7 68.1	F: ATTTCTGCCGGTCCACACTT R: CCATAGATCGGCCAACGACA
sod-2	67.5 65.9	F: GAGGCGGTCTCCAAAGGAAA R: GAACAGCCGACAGTTGATGCC
sod-3	63.9 64.0	F: GGATGGTGGAGAACCTTCAA R: AAGGATCCTGGTTTGCACAG
tba-1	66.4 67.4	F: AGACCAACAAGCCGATGGAG R: TCAGTTCCTTTCCGACGGTG
ugt-13	65.0 65.0	F: CCGGATTCCTGGATCGACTG R: TTGTCGCAGTAGTTGGGACC

References:

1. de Magalhães JP, Stevens M, Thornton D. The Business of Anti-Aging Science. Trends Biotechnol. 2017 Nov 1;35(11):1062–73.

2. New Data Shows Diabetes Rates And Economic Burden On Families Continue To Rise In Ontario [Internet]. DiabetesCanadaWebsite. [cited 2022 Nov 5]. Available from: https://www.diabetes.ca/media-room/press-releases/new-data-shows-diabetes-rates-and-economic-burden-on-families-continue-to-rise-in-ontario--

3. Chambers LW, Bancej C, McDowell I. Prevalence and Monetary Costs of Dementia in Canada. :70.

4. Finkel T. Signal transduction by reactive oxygen species. J Cell Biol. 2011 Jul 11;194(1):7–15.

5. Di Meo S, Reed TT, Venditti P, Victor VM. Harmful and Beneficial Role of ROS. Oxid Med Cell Longev. 2016;2016:7909186.

6. Trachootham D, Lu W, Ogasawara MA, Valle NRD, Huang P. Redox Regulation of Cell Survival. Antioxid Redox Signal. 2008 Aug;10(8):1343–74.

7. Weinberg F, Chandel NS. Reactive oxygen species-dependent signaling regulates cancer. Cell Mol Life Sci. 2009 Jul 24;66(23):3663.

8. Brenner S. The genetics of behaviour. Br Med Bull. 1973 Sep;29(3):269–71.

9. Reeve E. The Nematode *Caenorhabditis elegans*. Edited by William B. Wood and the Community of *C. elegans* Researchers. New York: Cold Spring Harbor Laboratory, 1988. 667 pages. US $97.00. ISBN 0 87969 307 X. Genet Res. 1988 Dec;52(3):243–4.

10. Riddle DL, Blumenthal T, Meyer BJ, Priess JR. The Biological Model [Internet]. *C. elegans* II. 2nd edition. Cold Spring Harbor Laboratory Press; 1997 [cited 2022 Oct 2]. Available from: https://www.ncbi.nlm.nih.gov/books/NBK20086/

11. Singson A. Every Sperm Is Sacred: Fertilization in *Caenorhabditis elegans*. Dev Biol. 2001 Feb;230(2):101–9.

12. *C. elegans* Sequencing Consortium. Genome sequence of the nematode *C. elegans*: a platform for investigating biology. Science. 1998 Dec 11;282(5396):2012–8.

13. Gerstein MB, Lu ZJ, Van Nostrand EL, Cheng C, Arshinoff BI, Liu T, et al. Integrative analysis of the *Caenorhabditis elegans* genome by the modENCODE project. Science. 2010 Dec 24;330(6012):1775–87.

14. Zhang Y, Zou X, Ding Y, Wang H, Wu X, Liang B. Comparative genomics and functional study of lipid metabolic genes in *Caenorhabditis elegans*. BMC Genomics. 2013 Mar 12;14(1):164.

15. Why study *C. elegans*? [Internet]. [cited 2022 Oct 30]. Available from: http://www.people.ku.edu/~erikl/Lundquist_Lab/Why_study_C._elegans.html

16. Ozougwu J. The Role of Reactive Oxygen Species and Antioxidants in Oxidative Stress. Int J Pharm Biosci. 2016 Jun 1;3:1–8.

17. Griendling KK, Sorescu D, Ushio-Fukai M. NAD (P) H oxidase: role in cardiovascular biology and disease. Circ Res. 2000;86(5):494–501.

18. Spiekermann S, Landmesser U, Dikalov S, Bredt M, Gamez G, Tatge H, et al. Electron spin resonance characterization of vascular xanthine and NAD(P)H oxidase activity in patients with coronary artery disease: relation to endothelium-dependent vasodilation. Circulation. 2003;107(10):1383–9.

19. Landmesser U, Dikalov S, Price SR, McCann L, Fukai T, Holland SM, et al. Oxidation of tetrahydrobiopterin leads to uncoupling of endothelial cell nitric oxide synthase in hypertension. J Clin Invest. 2003 Apr 15;111(8):1201–9.

20. Fridovich I. Mitochondria: are they the seat of senescence? Aging Cell. 2004;3(1):13–6.

21. Blackwell TK, Steinbaugh MJ, Hourihan JM, Ewald CY, Isik M. SKN-1/Nrf, stress responses, and aging in *Caenorhabditis elegans*. Free Radic Biol Med. 2015 Nov 1;88:290–301.

22. McCord JM, Fridovich I. Superoxide Dismutase: AN ENZYMIC FUNCTION FOR ERYTHROCUPREIN (HEMOCUPREIN). J Biol Chem. 1969 Nov 25;244(22):6049–55.

23. Hoogewijs D, Houthoofd K, Matthijssens F, Vandesompele J, Vanfleteren JR. Selection and validation of a set of reliable reference genes for quantitative sod gene expression analysis in *C. elegans*. BMC Mol Biol. 2008 Dec;9(1):9.

24. Cotgreave IA, Moldéus P, Brattsand R, Hallberg A, Andersson CM, Engman L. α-(Phenylselenenyl) acetophenone derivatives with glutathione peroxidase-like activity: A comparison with ebselen. Biochem Pharmacol. 1992 Feb 18;43(4):793–802.

25. van Bladeren PJ. Glutathione conjugation as a bioactivation reaction. Chem Biol Interact. 2000 Dec 1;129(1):61–76.

26. Yan F, Yang WK, Li XY, Lin TT, Lun YN, Lin F, et al. A trifunctional enzyme with glutathione S-transferase, glutathione peroxidase and superoxide dismutase activity. Biochim Biophys Acta. 2008 Jul 1;1780:869–72.

27. Hayflick L. How and why we age. Exp Gerontol. 1998 Dec;33(7–8):639–53.

28. Son HG, Altintas O, Kim EJE, Kwon S, Lee SV. Age-dependent changes and biomarkers of aging in *Caenorhabditis elegans*. Aging Cell. 2019 Apr;18(2):e12853.

29. Harman D. Aging: A Theory Based on Free Radical and Radiation Chemistry. Sci Aging Knowl Environ. 2002 Sep 18;2002(37):cp14–cp14.

30. Friedman DB, Johnson TE. A mutation in the *age-1* gene in *Caenorhabditis elegans* lengthens life and reduces hermaphrodite fertility. Genetics. 1988 Jan 1;118(1):75–86.

31. Kenyon C, Chang J, Gensch E, Rudner A, Tabtiang R. A *C. elegans* mutant that lives twice as long as wild type. Nature. 1993 Dec;366(6454):461–4.

32. Barsyte D, Lovejoy DA, Lithgow GJ. Longevity and heavy metal resistance in *daf-2* and age-1 long-lived mutants of *Caenorhabditis elegans*. FASEB J. 2001;15(3):627–34.

33. Prasad AS. Chapter 25 - Zinc, Oxidative Stress in the Elderly and Implications for Inflammation. In: Preedy VR, editor. Aging [Internet]. San Diego: Academic Press; 2014 [cited 2022 Oct 14]. p. 259–75. Available from: https://www.sciencedirect.com/science/article/pii/B9780124059337000251

34. Lee TI, Young RA. Transcriptional Regulation and its Misregulation in Disease. Cell. 2013 Mar 14;152(6):1237–51.

35. Reece-Hoyes JS, Deplancke B, Shingles J, Grove CA, Hope IA, Walhout AJ. A compendium of *Caenorhabditis elegans* regulatory transcription factors: a resource for mapping transcription regulatory networks. Genome Biol. 2005 Dec 30;6(13):R110.

36. Narasimhan K, Lambert SA, Yang AW, Riddell J, Mnaimneh S, Zheng H, et al. Mapping and analysis of *Caenorhabditis elegans* transcription factor sequence specificities. Friedman N, editor. eLife. 2015 Apr 23;4:e06967.

37. Wang R, Zhang S, Previn R, Chen D, Jin Y, Zhou G. Role of Forkhead Box O Transcription Factors in Oxidative Stress-Induced Chondrocyte Dysfunction: Possible Therapeutic Target for Osteoarthritis? Int J Mol Sci. 2018 Nov 28;19(12):3794.

38. Kim S, Shendure J. Mechanisms of Interplay between Transcription Factors and the 3D Genome. Mol Cell. 2019 Oct 17;76(2):306–19.

39. Lee SS, Kennedy S, Tolonen AC, Ruvkun G. DAF-16 Target Genes That Control *C. elegans* Life-Span and Metabolism. Science. 2003 Apr 25;300(5619):644–7.

40. Kimura KD, Tissenbaum HA, Liu Y, Ruvkun G. daf-2, an Insulin Receptor-Like Gene That Regulates Longevity and Diapause in *Caenorhabditis elegans*. Science. 1997 Aug 15;277(5328):942–6.

41. Tatar M, Kopelman A, Epstein D, Tu MP, Yin CM, Garofalo RS. A Mutant *Drosophila* Insulin Receptor Homolog That Extends Life-Span and Impairs Neuroendocrine Function. Science. 2001 Apr 6;292(5514):107–10.

42. Murphy CT, Hu PJ. Insulin/insulin-like growth factor signaling in *C. elegans* [Internet]. WormBook: The Online Review of *C. elegans* Biology [Internet]. WormBook; 2018 [cited 2022 Oct 14]. Available from: https://www.ncbi.nlm.nih.gov/books/NBK179230/

43. Murphy CT, McCarroll SA, Bargmann CI, Fraser A, Kamath RS, Ahringer J, et al. Genes that act downstream of DAF-16 to influence the lifespan of *Caenorhabditis elegans*. Nature. 2003 Jul;424(6946):277–83.

44. Calnan DR, Brunet A. The FoxO code. Oncogene. 2008 Apr;27(16):2276–88.

45. Tullet JMA, Hertweck M, An JH, Baker J, Hwang JY, Liu S, et al. Direct Inhibition of the Longevity-Promoting Factor SKN-1 by Insulin-like Signaling in *C. elegans*. Cell. 2008 Mar 21;132(6):1025–38.

46. Chiang WC, Ching TT, Lee HC, Mousigian C, Hsu AL. A complex containing DDL-1 and HSF-1 links insulin-like signaling to heat-shock response in *C. elegans*. Cell. 2012 Jan 20;148(1–2):322–34.

47. Chang L, Karin M. Mammalian MAP kinase signalling cascades. Nature. 2001 Mar 1;410(6824):37–40.

48. Sakaguchi A, Matsumoto K, Hisamoto N. Roles of MAP Kinase Cascades in *Caenorhabditis elegans*. J Biochem (Tokyo). 2004 Jul 1;136(1):7–11.

49. Plotnikov A, Zehorai E, Procaccia S, Seger R. The MAPK cascades: Signaling components, nuclear roles and mechanisms of nuclear translocation. Biochim Biophys Acta BBA - Mol Cell Res. 2011 Sep 1;1813(9):1619–33.

50. Sundaram M, Han M. Control and integration of cell signaling pathways during *C. elegans* vulval development. BioEssays. 1996;18(6):473–80.

51. Szewczyk N, Jacobson L. Activated EGL-15 FGF receptor promotes protein degradation in muscles of *Caenorhabditis elegans*. EMBO J. 2003 Nov 1;22:5058–67.

52. Hirotsu T, Saeki S, Yamamoto M, Iino Y. The Ras-MAPK pathway is important for olfaction in *Caenorhabditis elegans*. Nature. 2000 Mar;404(6775):289–93.

53. Lemmon MA, Schlessinger J. Cell signaling by receptor tyrosine kinases. Cell. 2010 Jun 25;141(7):1117–34.

54. Karnoub AE, Weinberg RA. Ras oncogenes: split personalities. Nat Rev Mol Cell Biol. 2008 Jul;9(7):517–31.

55. Udell CM, Rajakulendran T, Sicheri F, Therrien M. Mechanistic principles of RAF kinase signaling. Cell Mol Life Sci CMLS. 2011 Feb;68(4):553–65.

56. Yoon S, Seger R. The extracellular signal-regulated kinase: multiple substrates regulate diverse cellular functions. Growth Factors Chur Switz. 2006 Mar;24(1):21–44.

57. Okuyama T, Inoue H, Ookuma S, Satoh T, Kano K, Honjoh S, et al. The ERK-MAPK Pathway Regulates Longevity through SKN-1 and Insulin-like Signaling in *Caenorhabditis elegans**. J Biol Chem. 2010 Sep 24;285(39):30274–81.

58. Kawasaki M, Hisamoto N, Iino Y, Yamamoto M, Ninomiya-Tsuji J, Matsumoto K. A *Caenorhabditis elegans* JNK signal transduction pathway regulates coordinated movement via type-D GABAergic motor neurons. EMBO J. 1999 Jul;18(13):3604–15.

59. Oh SW, Mukhopadhyay A, Svrzikapa N, Jiang F, Davis RJ, Tissenbaum HA. JNK regulates lifespan in *Caenorhabditis elegans* by modulating nuclear translocation of forkhead transcription factor/DAF-16. Proc Natl Acad Sci U S A. 2005 Mar 22;102(12):4494–9.

60. Inoue H, Hisamoto N, An JH, Oliveira RP, Nishida E, Blackwell TK, et al. The *C. elegans* p38 MAPK pathway regulates nuclear localization of the transcription factor SKN-1 in oxidative stress response. Genes Dev. 2005 Oct 1;19(19):2278–83.

61. Kim DH, Feinbaum R, Alloing G, Emerson FE, Garsin DA, Inoue H, et al. A Conserved p38 MAP Kinase Pathway in *Caenorhabditis elegans* Innate Immunity. Science. 2002 Jul 26;297(5581):623–6.

62. Chan JY, Han XL, Kan YW. Cloning of Nrf1, an NF-E2-related transcription factor, by genetic selection in yeast. Proc Natl Acad Sci U S A. 1993 Dec 1;90(23):11371–5.

63. Isolation of NF-E2-related factor 2 (Nrf2), a NF-E2-like basic leucine zipper transcriptional activator that binds to the tandem NF-E2/AP1 repeat of the beta-globin locus control region. [Internet]. [cited 2022 Oct 23]. Available from: https://www.pnas.org/doi/10.1073/pnas.91.21.9926

64. Kobayashi A, Ito E, Toki T, Kogame K, Takahashi S, Igarashi K, et al. Molecular Cloning and Functional Characterization of a New Cap'n' Collar Family Transcription Factor Nrf3 *. J Biol Chem. 1999 Mar 5;274(10):6443–52.

65. Isolation of cDNA encoding the human NF-E2 protein. | PNAS [Internet]. [cited 2022 Oct 23]. Available from: https://www.pnas.org/doi/abs/10.1073/pnas.90.23.11366

66. He F, Ru X, Wen T. NRF2, a Transcription Factor for Stress Response and Beyond. Int J Mol Sci. 2020 Jul 6;21(13):4777.

67. Nguyen T, Sherratt PJ, Pickett CB. Regulatory mechanisms controlling gene expression mediated by the antioxidant response element. Annu Rev Pharmacol Toxicol. 2003;43:233–60.

68. Motohashi H, O'Connor T, Katsuoka F, Engel JD, Yamamoto M. Integration and diversity of the regulatory network composed of Maf and CNC families of transcription factors. Gene. 2002 Jul 10;294(1):1–12.

69. Mitsuishi Y, Motohashi H, Yamamoto M. The Keap1-Nrf2 system in cancer: Stress response and anabolic metabolism. Front Oncol. 2012 Dec 26;2:200.

70. Blackwell TK, Bowerman B, Priess JR, Weintraub H. Formation of a Monomeric DNA Binding Domain by Skn-1 bZIP and Homeodomain Elements. Science. 1994 Oct 28;266(5185):621–8.

71. Walker AK, See R, Batchelder C, Kophengnavong T, Gronniger JT, Shi Y, et al. A Conserved Transcription Motif Suggesting Functional Parallels between *Caenorhabditis elegans* SKN-1 and Cap'n'Collar-related Basic Leucine Zipper Proteins. J Biol Chem. 2000 Jul;275(29):22166–71.

72. Leung CK, Hasegawa K, Wang Y, Deonarine A, Tang L, Miwa J, et al. Direct interaction between the WD40 repeat protein WDR-23 and SKN-1/Nrf inhibits binding to target DNA. Mol Cell Biol. 2014;34(16):3156–67.

73. Mcmahon M, Thomas N, Itoh K, Yamamoto M, Hayes J. Redox-regulated Turnover of Nrf2 Is Determined by at Least Two Separate Protein Domains, the Redox-sensitive Neh2 Degron and the Redox-insensitive Neh6 Degron. J Biol Chem. 2004 Aug 1;279:31556–67.

74. Lehrbach NJ, Breen PC, Ruvkun G. Protein sequence editing of SKN-1A/Nrf1 by peptide:N-glycanase controls proteasome gene expression. Cell. 2019 Apr 18;177(3):737-750.e15.

75. This reference has been removed.

76. Bishop NA, Guarente L. Two neurons mediate diet-restriction-induced longevity in *C. elegans*. Nature. 2007 May;447(7144):545–9.

77. Glover-Cutter K, Lin S, Blackwell TK. Integration of the Unfolded Protein and Oxidative Stress Responses through SKN-1/Nrf. PLoS Genet. 2013 Sep 1;9:e1003701.

78. An JH, Blackwell TK. SKN-1 links *C. elegans* mesendodermal specification to a conserved oxidative stress response. Genes Dev. 2003 Aug 1;17(15):1882–93.

79. Choe KP, Przybysz AJ, Strange K. The WD40 Repeat Protein WDR-23 Functions with the CUL4/DDB1 Ubiquitin Ligase To Regulate Nuclear Abundance and Activity of SKN-1 in *Caenorhabditis elegans*. Mol Cell Biol. 2009 May 15;29(10):2704–15.

80. Oliveira RP, Abate JP, Dilks K, Landis J, Ashraf J, Murphy CT, et al. Condition-adapted stress and longevity gene regulation by *Caenorhabditis elegans* SKN-1/Nrf. Aging Cell. 2009;8(5):524–41.

81. Hu Q, D'Amora DR, MacNeil LT, Walhout AJM, Kubiseski TJ. The Oxidative Stress Response in *Caenorhabditis elegans* Requires the GATA Transcription Factor ELT-3 and SKN-1/Nrf2. Genetics. 2017 Aug;206(4):1909–22.

82. Li S, Ku CY, Farmer AA, Cong YS, Chen CF, Lee WH. Identification of a Novel Cytoplasmic Protein That Specifically Binds to Nuclear Localization Signal Motifs*. J Biol Chem. 1998 Mar 13;273(11):6183–9.

83. Matheny SA, Chen C, Kortum RL, Razidlo GL, Lewis RE, White MA. Ras regulates assembly of mitogenic signalling complexes through the effector protein IMP. Nature. 2004 Jan;427(6971):256–60.

84. Stewart S, Sundaram M, Zhang Y, Lee J, Han M, Guan KL. Kinase Suppressor of Ras Forms a Multiprotein Signaling Complex and Modulates MEK Localization. Mol Cell Biol. 1999 Aug;19(8):5523–34.

85. Koon JC, Kubiseski TJ. Developmental Arrest of *Caenorhabditis elegans* BRAP-2 Mutant Exposed to Oxidative Stress Is Dependent on BRC-1*. J Biol Chem. 2010 Apr 30;285(18):13437–43.

86. Kolch W. Coordinating ERK/MAPK signalling through scaffolds and inhibitors. Nat Rev Mol Cell Biol. 2005 Nov;6(11):827–37.

87. Accili D, Arden KC. FoxOs at the Crossroads of Cellular Metabolism, Differentiation, and Transformation. Cell. 2004 May 14;117(4):421–6.

88. Albert PS, Brown SJ, Riddle DL. Sensory control of dauer larva formation in *Caenorhabditis elegans*. J Comp Neurol. 1981;198(3):435–51.

89. Riddle DL, Albert PS. Genetic and Environmental Regulation of Dauer Larva Development. In: Riddle DL, Blumenthal T, Meyer BJ, Priess JR, editors. C elegans II [Internet]. 2nd ed. Cold Spring Harbor (NY): Cold Spring Harbor Laboratory Press; 1997 [cited 2022 Oct 26]. Available from: http://www.ncbi.nlm.nih.gov/books/NBK20018/

90. Albert PS, Brown SJ, Riddle DL. Sensory control of dauer larva formation in *Caenorhabditis elegans*. J Comp Neurol. 1981 May 20;198(3):435–51.

91. Mukhopadhyay A, Oh SW, Tissenbaum HA. Worming pathways to and from DAF-16/FOXO. Exp Gerontol. 2006 Oct;41(10):928–34.

92. Hertweck M, Göbel C, Baumeister R. *C. elegans* SGK-1 is the critical component in the Akt/PKB kinase complex to control stress response and life span. Dev Cell. 2004 Apr;6(4):577–88.

93. Lin K, Hsin H, Libina N, Kenyon C. Regulation of the *Caenorhabditis elegans* longevity protein DAF-16 by insulin/IGF-1 and germline signaling. Nat Genet. 2001 Jun;28(2):139–45.

94. Hsin H, Kenyon C. Signals from the reproductive system regulate the lifespan of *C. elegans*. Nature. 1999 May;399(6734):362–6.

95. Robida-Stubbs S, Glover-Cutter K, Lamming DW, Mizunuma M, Narasimhan SD, Neumann-Haefelin E, et al. TOR Signaling and Rapamycin Influence Longevity by Regulating SKN-1/Nrf and DAF-16/FoxO. Cell Metab. 2012 May 2;15(5):713–24.

96. Tullet JMA, Araiz C, Sanders MJ, Au C, Benedetto A, Papatheodorou I, et al. DAF-16/FoxO Directly Regulates an Atypical AMP-Activated Protein Kinase Gamma Isoform to Mediate the Effects of Insulin/IGF-1 Signaling on Aging in *Caenorhabditis elegans*. PLOS Genet. 2014 Feb 6;10(2):e1004109.

97. Sun X, Chen WD, Wang YD. DAF-16/FOXO Transcription Factor in Aging and Longevity. Front Pharmacol [Internet]. 2017 [cited 2022 Dec 20];8. Available from: https://www.frontiersin.org/articles/10.3389/fphar.2017.00548

98. Gommans WM, Haisma HJ, Rots MG. Engineering Zinc Finger Protein Transcription Factors: The Therapeutic Relevance of Switching Endogenous Gene Expression On or Off at Command. J Mol Biol. 2005 Dec 2;354(3):507–19.

99. DM Z, LL P, EM M. Interaction of primary amines with a mixed-function amine oxidase isolated from pig liver microsomes. Xenobiotica. 1971 Jul 1;1(4):523–31.

100. Mackay JP, Crossley M. Zinc fingers are sticking together. Trends Biochem Sci. 1998 Jan;23(1):1–4.

101. Hodgkin JA, Brenner S. Mutations Causing Transformation of Sexual Phenotype in the nematode *Caenorhabditis elegans*. Genetics. 1977 Jun 1;86(2):275–87.

102. Grote P, Conradt B. The PLZF-like Protein TRA-4 Cooperates with the Gli-like Transcription Factor TRA-1 to Promote Female Development in *C. elegans*. Dev Cell. 2006 Oct 1;11(4):561–73.

103. Uil TG, Haisma HJ, Rots MG. Therapeutic modulation of endogenous gene function by agents with designed DNA-sequence specificities. Nucleic Acids Res. 2003 Nov 1;31(21):6064–78.

104. Brenner S. The Genetics of *Caenorhabditis elegans*. Genetics. 1974 May 1;77(1):71–94.

105. introfig1.jpg (2480×1548) [Internet]. [cited 2022 Nov 22]. Available from: https://www.wormatlas.org/hermaphrodite/introduction/IMAGES/introfig1.jpg

106. Detienne G, Van de Walle P, De Haes W, Schoofs L, Temmerman L. SKN-1-independent transcriptional activation of glutathione S-transferase 4 (GST-4) by EGF signaling. Worm. 2016 Aug 31;00–00.

107. Mitchell RA, Chang BF, Huang CH, DeMaster EG. Inhibition of mitochondrial energy-linked functions by arsenate. Evidence for a nonhydrolytic mode of inhibitor action. Biochemistry. 1971 May 1;10(11):2049–54.

108. Mathews WR, Guido DM, Fisher MA, Jaeschke H. Lipid peroxidation as molecular mechanism of liver cell injury during reperfusion after ischemia. Free Radic Biol Med. 1994 Jun 1;16(6):763–70.

109. Poulsen LL, Masters BS, Ziegler DM. Mechanism of 2-naphthylamine oxidation catalysed by pig liver microsomes. Xenobiotica Fate Foreign Compd Biol Syst. 1976 Aug;6(8):481–98.

110. Poulsen LL, Ziegler DM. The liver microsomal FAD-containing monooxygenase. Spectral characterization and kinetic studies. J Biol Chem. 1979 Jul;254(14):6449–55.

111. Huang S, Howington MB, Dobry CJ, Evans CR, Leiser SF. Flavin-containing monooxygenases are conserved regulators of stress resistance and metabolism. Frontiers in Cell and Developmental Biology. 2021 Feb 12;9:630188.

112. Lin K, Dorman JB, Rodan A, Kenyon C. daf-16: An HNF-3/forkhead Family Member That Can Function to Double the Life-Span of *Caenorhabditis elegans*. Science. 1997 Nov 14;278(5341):1319–22.

113. Schröder M. Endoplasmic reticulum stress responses. Cell Mol Life Sci. 2008 Mar;65(6):862–94.

114. WormBase : Nematode Information Resource [Internet]. [cited 2022 Dec 20]. Available from: https://wormbase.org/#012-34-5